Abstract

We propose a Bayesian VAR model with stochastic volatility and time varying skewness to estimate the degree of labour at risk in the euro area and in the United States. We model the asymmetry of the shocks to changes in the unemployment rate as a function of real activity and financial risk factors. We find that the conditional distribution of the changes in the unemployment rate displays time-varying volatility and skewness, with peaks coinciding with the Global Financial Crisis and the COVID-19 pandemic. We take advantage of the multivariate nature of our parametric model to measure stagflation risk defined as the possible joint event of large increases in the unemployment rate and large annual rates of inflation. We find an increasing risk of stagflation for the euro area in 2022 while in the United States stagflation risk increased earlier in 2021 and started decreasing more recently. Notwithstanding the significantly high levels of inflation, stagflation risks have been contained by the resilient performance of the labour market in both areas. The degree of labour at risk is therefore important for the assessment of the inflation-unemployment trade-off.

Non-Technical Summary

The cyclical asymmetry of business cycles is a longstanding topic in the economic literature and key to this idea is the fact that, on average, contractions in economic activity are briefer and more violent than economic expansions. For the labour market, this implies that the number of persons losing their jobs and becoming unemployed rises abruptly during recessions. These persons only slowly get back into employment, leading to the unemployment rate decreasing at a slower pace during economic expansions. More generally, the cyclical asymmetry in the labour market can be related to the assessment of tail risks. These tail risks can account for possible worst case scenarios that could occur in case of economic downturns. Hence, the assessment of tail risks merits the attention of policymakers, who attempt via their policy actions to mitigate some of the welfare losses arising in case a recession occurs and the tail risks are realised.

We tackle this topic from a quantitative perspective and estimate the degree of tail risks in the labour market (i.e., "labour at risk") at any given point in time both in the euro area and in the United States. We estimate the probability of the unemployment rate suddenly and violently increasing over time for both geographical areas. We use an augmented version of our model to assess the joint risk of having simultaneously large increases in the unemployment rate and large annual inflation rates, which we denote as the risk of stagflation.

We track an increasing risk of stagflation in the euro area in 2022. Our results suggest that stagflation risk has been limited by the resilient performance of the euro area labour market. However, our measure of labour at risk has increased during 2022 in the euro area. The risk of stagflation in the euro area is expected to reach in December 2022 similar levels to those reached during the Global Financial Crisis, although then it was triggered by an increase in labour at risk as the risk of inflation was being contained. For the US, the risk of stagflation increased during 2021 and decreased in 2022 given the robust performance of the labour market. By contrast to the results for the euro area, the risk of stagflation in the US remained considerably more contained than during the Global Financial Crisis.

These results motivate the use of our model to track the joint risk of stagflation in both the euro area and in the US and its main channels. We find that labour at risk and inflation at risk usually occur at different points in time, with a higher degree of labour at risk tending to follow a higher inflation at risk. The timing of these risks could provide important for the assessment of the inflation-unemployment trade-off and on the role for (and action of) monetary policy.

1 Introduction

The cyclical asymmetry of business cycles is a longstanding topic in the economic literature, which can be traced back to Mitchell (1927) and Keynes (1936). Key to this idea is the fact that, on average, contractions in economic activity are briefer and more violent than economic expansions. The asymmetry of cyclical developments is historically salient in the labour market, being identified using both the unemployment rate (Neftçi (1984), DeLong et al. (1986), Falk (1986)) and total employment (McKay et al. (2008), Ferraro et al. (2022)). The number of persons losing their jobs and becoming unemployed rises abruptly during recessions. Conversely, unemployed workers take their time to slowly get back into employment, with the unemployment rate decreasing (or employment increasing) at a slower pace during economic expansions.

More generally, the cyclical asymmetry in the labour market can be related to the assessment of tail risks. These tail risks can be estimated to account for the possible worst case scenarios that could occur in case of economic downturns. Hence, the assessment of tail risks merits the attention of policymakers, who attempt via their policy actions to mitigate some of the welfare losses arising in case a recession occurs and the tail risks are realised.

In this paper, we tackle this topic from a quantitative perspective and estimate the degree of tail risks in the labour market at any given point in time both in the euro area and in the United States. To do so, we propose a fully parametric econometric model with skew-normal shocks featuring both stochastic volatility and stochastic skewness. Our formulation is part of the more general class of Bayesian VAR (BVAR) models with stochastic volatility and time varying skewness discussed in Renzetti (2023). We use this model to extract out-of-sample forecasts that allow us to monitor the degree of "labour-at-risk" and the probability of large increases in the unemployment rate over time. We take advantage of the multivariate nature of our parametric model to measure stagflation-risk both the euro area and the US, which we define as the possible joint event of large increases in the unemployment rate and large annual rates of inflation.

There are several channels that could be behind the cyclical asymmetry of the labour market. On the one hand, it is important to quantify the relationship between the cyclical developments in real activity, which can be symmetric or not, and those in the labour market. For example, in the standard "DMP" model with search and matching frictions (Diamond (1982), Mortensen (1982), Pissarides (1985)), shocks to labour productivity can drive the asymmetry in the unemployment rate via asymmetric fluctuations in the rate of job destruction (Andolfatto (1997)). This implies

that even when the business cycles are symmetric, the economy can be faced with sudden and large increases in unemployment during recessions. This could indicate that the Okun's law breaks down during recessions or is at the very least non-linear and state-dependent.

On the other hand, external frictions can simultaneously make both the real output and the labour market to be asymmetric. For example, downward nominal wage rigidities in New Keynesian models inhibit the necessary real wage cuts needed during recessions, thus leading to stronger declines in vacancy posting and employment during downturns than in models featuring symmetric wage adjustment costs (Abbritti et al. (2013)). Also, financial frictions could also induce skewed business cycles, by magnifying the impact of a downturn while leading to a more gradual recovery in a learning model by restricting information after the crisis (Ordoñez (2013)).[1]

We embed these mechanisms in our BVAR model by considering a specification at the monthly time frequency with the changes in the unemployment rate, a variable proxying for changes in real activity (the PMI output for the euro area and the CFNAI for the US), and a measure proxying for changes in financial conditions (the CISS indicator for the euro area and the NFCI for the US). By doing so, we allow the unemployment rate to move either driven by shocks specific to the labour market, as a response to shocks to real activity in a standard Okun's law framework, or as a response to large variations in financial conditions.

We allow for the skewness of the shocks specific to the labour market to be state dependent, increasing when real activity slows down and financial conditions tighten. In simple terms, the labour market is more likely to be faced with strong adverse shocks that increase the unemployment rate substantially when the economy is in a bad state of the world. This bad state of the world can vary between a very sharp slow down of the economy or a prolonged recession for real activity, or instead a strong tightening of financial conditions. This implies that during bad states of the world, shocks to the monthly changes in the unemployment rate become asymmetric and right-skewed, meaning that large increases in the unemployment rate become more likely in these periods than in good times. By allowing the distribution of the shocks to the unemployment rate to shift as a function of (lagged) real activity and financial risk factors, the model is in this way able to capture possible non-linear relationships between real activity and the labour market, and to cater for the role of financial frictions. We find also that the

---

1. Regarding alternative mechanisms we highlight, for example, the role of worker-level heterogeneity in models with search and matching frictions in matching the asymmetric response of the employment rate to shocks over the business cycle (Ferraro (2018)). We notice also that micro-level evidence points towards firms following concave hiring rules, making them slower to hire after good shocks and quicker to fire after bad shocks (Ilut et al. (2018)).

skewness of the shocks to the changes in the unemployment rate varies over the business cycle, increasing and often peaking during economic downturns, and it increases (or decreases) as the systemic financial stress conditions deteriorate (or improve).

Our paper is related to the growing strand of literature aimed at assessing and quantifying tail risk to macroeconomic outcomes. Methodologically, this literature traditionally relies on quantile regression based methods, such as those used by Giglio et al. (2016) and Adrian et al. (2019). Most of the literature on the assessment of tail risks to macroeconomic outcomes focus uniquely on output growth and inflation. Considerably less attention has been devoted to the analysis of tail risks in the labour market. The exception is Kiley (2022), who provides an assessment of tail risks to the US unemployment rate using quantile regressions.

We depart away from quantile regressions and propose a fully parametric model to assess tail risks in the labour market. In this sense, our work is more closely linked to a recent strand in the literature that proposes the usage of fully parametric models to assess and predict tail risks, as in López-Salido et al. (2020), Plagborg-Møller et al. (2020), Carriero et al. (2020a), Carriero et al. (2020b), Delle Monache et al. (2021), Brownlees et al. (2021), Wolf (2021), Iseringhausen (2023), or Montes-Galdón et al. (2022), to provide some examples. Similarly to our own contribution, this strand of literature argues that fully parametric models are more flexible than quantile regression based methods, while simultaneously achieving a similar forecasting performance.[2] Moreover, we are able to further extend the model and incorporate also information on inflation rates. We use the augmented setup to assess the joint risk of having simultaneously large increases in the unemployment rate and large annual inflation rates.

We find a similar result in our application to the euro area or US labour markets. In particular, our BVAR with stochastic volatility and time varying skewness displays a forecasting performance that is at least as good as, but often superior in terms of density forecast accuracy to other benchmarks including the quantile regression based methods from Adrian et al. (2019), a standard BVAR model, and a BVAR model with stochastic volatility.

---

2. It should be noted that both Wolf (2021) and Iseringhausen (2023) employ also stochastic volatility models with asymmetric shocks and stochastic skewness. However, both models are univariate. Our model is multivariate and allows to jointly model the dynamic relationship between the risk factors and the target variables. As well the multivariate nature of our model allows us to assess tail risk to multiple target variables (unemployment rate and inflation). Relatedly, Chavleishvili et al. (2019) extend the quantile regression based methods to a quantile VAR (QVAR) model framework. This methodology allows to model the interaction between any quantiles of the endogenous variables. The increased flexibility comes at the cost of highly complex modelling assumptions and estimation algorithm. For this reason, we leave the comparison of the forecasting performance and labour-at-risk measurement between our application and a QVAR model for the labour market for future research.

This paper is organised as follows. Section 2 describes the data we use and the main features of the unemployment rate, which motivate our modelling choice to assess tail risks. Section 3 describes our BVAR model with stochastic volatility and time varying skewness, and our application of this model to tackle the cyclical asymmetry in the labour market. Section 4 presents most of our empirical results, focusing first on the in-sample assessment of the model, then on the construction of our "labour-at-risk" measure, and finally on the out-of-sample forecasting performance of the model. Section 5 extends our BVAR model application to assess probabilities and risk of joint events, applied to measuring the risk of stagflation. Section 6 concludes.

2 Data description

We work with monthly data from January 1999 to September 2022 for the euro area and from January 1971 to September 2022 for the United States. For both regions, we use the unemployment rate to account for the conditions of the labour market and two risk factors: (i) a monthly indicator for real economic activity, which allows us to account for the reaction of the labour market as a response to changes in economic activity; and (ii) a monthly indicator for financial conditions, which we use to cater for the role of financial frictions in shaping movements in real activity and in the labour market.

For the euro area, the unemployment rate is obtained from the ECB Statistical Data Warehouse. We use the Purchasing Manager Index (PMI) Output from S&P Global to proxy for the developments in real activity.[3] This indicator tracks the assessments by corporate executives regarding the immediate reactions of their firms to idiosyncratic events over time, and contain in this way information on the cyclical developments in real activity. As proxy for financial conditions we use the Composite Indicator of Systemic Stress (CISS), which is the most widely used indicator for financial conditions in the euro area in the literature assessing tail risks to macroeconomic outcomes (Kremer et al. (2012), Figueres et al. (2020)). This indicator aims to track the current level of frictions, stresses and strains in the financial system. It is available at daily frequency and we obtain a monthly series by averaging over the daily observations.

For the United States, we calculate the unemployment rate in two steps. First, we construct

---

3. As a robustness check, we consider instead the Eurocoin indicator provided by the Bank of Italy as a proxy for real activity. From a qualitatively point of view our results do not change. For space considerations, we do not report the results in the text, although they can be provided upon request. We decided to use the PMI output as it allows for a better forecasting performance to our empirical application.

the number of unemployed workers by obtaining the difference between the civilian labour force and the civilian employment. We then construct the unemployment rate as the ratio between this measure of unemployment and the civilian labour force.[4] To proxy for the developments in real economic activity, we use the National Activity Index provided by the Federal Reserve of Chicago (CFNAI), which compares the growth rate of the economy to its historical trend. To gauge the state of financial conditions in the US, we borrow from the growth-at-risk literature, and use the National Financial Conditions Index (NFCI) from the Federal Reserve of Chicago, which is comparable in scope to the CISS indicator for the euro area. Both the CFNAI and the NFCI indicators are available at a weekly time frequency. Therefore, we aggregate the weekly observations each month by taking their average over the month.

Figure 1 for the euro area and Figure 2 for the US show the time series of the month on month changes in the unemployment rate together with the selected real activity and financial conditions indicators. Both figures show that the unemployment rate is more likely to display larger and more persistent increases when economic activity slows down considerably or financial conditions tighten substantially, suggesting that both indicators are informative on the magnitude and (a)symmetry of the monthly changes in the unemployment rate over time that we analyze in detail in the next paragraph.

[Figure 1 about here.]

[Figure 2 about here.]

2.1 Asymmetry of changes in the unemployment rate

The unemployment rate in the euro area decreased by almost four percentage points between April 1998 and September 2022. However, the long-term decline in the unemployment rate did not happen at a constant pace over time. The unemployment rate tends to decrease during expansions and to increase during recessions with the speed of changes in the unemployment rate depending on the state of the business cycles. In Table 1, we show the peak-to-trough (downturns) and trough-to-peak (expansions) changes in the unemployment rate in the euro area. In expansions, the unemployment rate decreased mildly by between -0.03 and -0.06 percentage

---

4. We obtain data on civilian employment and labor force from the FRED-MD database, provided by the Federal Reserve Bank of St. Louis. The source code for the civilian employment is LNS12000000 (or alternatively CE16OV), while for the civilian labour force is LNS11000000 (or alternatively CLF16OV).

points per month. The euro area unemployment rate even increased slightly in the expansion between the end of the Global Financial Crisis in 2009 Q2 and the start of the Sovereign Debt Crisis in 2011 Q3. By contrast, the unemployment rate increased at a more pronounced pace during recessions, rising on average by between 0.09 and 0.16 percentage points per month. This pattern also implies that the unconditional distribution of the changes in the euro area unemployment rate is skewed to the right (see Figure 3).

[Table 1 about here.]

The longer time series data for the United States shows a more cyclical unemployment rate than that observed for the euro area. By September 2022, the US unemployment rate was at levels broadly comparable to those observed in 1948. However, the US unemployment rate displays a similar cyclical asymmetry to that of the euro area. Economic expansions are linked with small average decreases in the unemployment rate on a magnitude of -0.06 percentage points per month. Not considering the current expansion following the COVID-19 pandemic, this average monthly decrease in the unemployment rate would be even milder, at -0.04 percentage points per month. By contrast, the US unemployment rate increases considerably faster during contractions at an average of 0.34 percentage points per month, or at 0.25 percentage points when we exclude the COVID-19 pandemic contraction. These results also imply that the unconditional distribution of the month-on-month changes in the US unemployment rate is markedly skewed to the right (see Figure 4), similarly to that observed for the euro area.

[Figure 3 about here.]

[Figure 4 about here.]

Hence, in both regions downturns are considerably shorter than upturns. These results taken together confirm that contractions are briefer and more violent than expansions in the euro area and the US labour markets. They also imply that the risks around the unemployment rate outlook are not symmetric, as the likelihood of large increases in the unemployment rate has been historically higher than the likelihood of large decreases. The steepness of the monthly changes in the unemployment rate is also visible when we extract the residuals from an autoregressive model regression to account for potential dynamic or slower movements in the unemployment rate over time. Both in the euro area and in the US, the symmetry of the residuals changes over time, with the residuals more right skewed during recessions than during expansions.

In more technical terms, we use the normality test proposed by Bai et al. (2005) to assess the skewness of the changes in the unemployment rate in both the euro area and in the US. [5] We calculate this statistic for the month-on-month, quarter-on-quarter, and year-on-year changes in the unemployment rate, and also to the level of the unemployment rate. We report the results of this test in Table 2 for our final sample from January 1999 to September 2022 for the euro area and from January 1971 to September 2022 for the United States.

[Table 2 about here.]

The skewness statistic from Bai et al. (2005) rejects the normality of both the month-on-month and quarter-on-quarter changes in the unemployment rate in the euro area, and it rejects the normality of the unemployment rate levels in the US. Both results highlight that there is cyclical asymmetry in the unemployment rate. For the United States, the adjustment of the unemployment rate during the COVID-19 pandemic and ensuing recovery exhibited a set of outliers that shifted the skewness statistic. When applied to the sample ending in December 2019, we find also a statistically significant skewness for the month-on-month changes in the US unemployment rate.

More generally, we find that the skewness of the changes in the unemployment rate is time-varying in both the euro area and the US. To showcase this, we compute the skewness statistic from Bai et al. (2005) for the distribution of the month-on-month changes in the unemployment rate on an expanding recursive window that comprises the first eight years of data for each region and adds one month of data at the time before calculating again the skewness statistic. The skewness statistics for the expanding windows are reported for the euro area in Figure 5 and for the United States in Figure 6. In September 2022, the expanding window covers the full sample and mimics the results in Table 2. For the euro area, the skewness statistic started very low and increases to a high level close to the 90% confidence band over the entire sample. Skewness becomes statistically significant in the euro area with the onset of the COVID-19 pandemic, with the skewness statistics increasing outside the 90% confidence interval.

[Figure 5 about here.]

[Figure 6 about here.]

5. Details on how the statistic is computed can be found in the Appendix A.1

The time variation in the skewness of the month-on-month changes in the unemployment rate is even more prevalent in the US. The skewness statistic is statistically significant during the period comprising the oil prices shocks and the Volcker's recession in the late 1970s and early 1980s, and then again following the Global Financial Crisis. The COVID-19 pandemic shifted the skewness statistic because of the unique timing and magnitudes of the monthly changes in the unemployment rate. As shown in Table 1, the unemployment rate increased by 5.6 percentage points per month between February 2020 and April 2020 and it decreased at a faster pace from May 2020 onwards over a relatively longer period of time. These results mark the importance of catering for the time-variation in the skewness of the unemployment rate in a time series modelling approach and provides the main motivation for our empirical model in the next section.

3 Model

3.1 Time varying skewness stochastic volatility VAR model

The time varying asymmetry of the unemployment rate leads to time varying tail risks that should be considered by any model that attempts to predict any future dynamics in the labour market. In this section we propose a fully parametric econometric model to provide a meaningful characterisation of tail risk in the labour market both the euro area and the United States.

Our model is a standard VAR model equipped with stochastic volatility and skew normal shocks.[6] These additional features are designed to capture both shifts in the volatility and in the skewness of the shocks to the endogenous variables in the VAR. The exact specification is:

$$\boldsymbol{y_t} = \boldsymbol{\Pi_0} + \boldsymbol{\Pi_1 y_{t-1}} + \ldots + \boldsymbol{\Pi_p y_{t-p}} + \boldsymbol{A^{-1} H_t^{0.5} \varepsilon_t} \tag{1}$$

$$\varepsilon_{it} \sim Skew\ normal(\zeta_{it}, \omega_{it}, \lambda_{it})$$

where $\boldsymbol{y_t}$ is the vector of endogenous variables, for $t = 1, \ldots, T$ periods (months). As endogenous variables, we consider the month-on-month changes in the unemployment rate, a monthly real activity indicator, the PMI output for the euro area and the CFNAI for the US, and a monthly indicator for financial conditions, the CISS indicator for the euro area and the NFCI for the US.

6. This class of models is comprehensively covered in Renzetti (2023), with an application for the "growth-at-risk" literature.

$\boldsymbol{A^{-1}}$ is a lower triangular matrix with ones on the main diagonal, $\boldsymbol{H_t} = diag(h_{1,t}, \ldots, h_{N,t})$ is the diagonal matrix collecting the volatilities of the shocks and $\boldsymbol{\varepsilon_t}$ is a column vector collecting the skew normal (as in Azzalini (1986)) shocks ε_{it} with $i = 1, \ldots, N$, and N being the number of endogenous variables.

In general the shape parameter λ_{it} shifts both the mean and the variance of skew normal distribution. To interpret ε_{it} as structural shocks in the VAR model, we then re-parametrize the skew normal distribution parameters ζ_{it} and ω_{it} such that $\mathbb{E}[\boldsymbol{\varepsilon_t}] = \boldsymbol{0_N}$ and $\mathbb{E}[\boldsymbol{\varepsilon_t \varepsilon_t'}] = \boldsymbol{I_N}$. That is, we ensure that the elements in $\boldsymbol{\varepsilon_t}$ are unpredictable in terms of their mean and that they have unit variance. This ensures as well that the elements on the diagonal matrix $\boldsymbol{H_t}$ provide the sufficient information on the variances of the shocks while the shape parameters λ_{it} carry sufficient information on the skewness of the shocks. In more detail, this re-parameterization implies the following constraints on the location and scale parameters of the shocks:

$$\zeta_{i,t} = -\omega_{i,t}\delta_{i,t}\sqrt{\frac{2}{\pi}} \qquad \forall i, t \tag{2}$$

$$\omega_{i,t}^2 = \left[1 - \frac{2}{\pi}\delta_{i,t}^2\right]^{-1} \qquad \forall i, t \tag{3}$$

where $\delta_{i,t} = \frac{\lambda_{i,t}}{\sqrt{1+\lambda_{i,t}^2}}$, with $-1 < \delta_{i,t} < 1$. The re-parametrised skew normal shocks are identified and interpreted as structural shocks assuming the short run restrictions implied by the ordering of the variables in the model (Cholesky identification).[7] We order the financial conditions indicator last, so as to allow financial markets to adjust within the month to shocks to real activity and to the unemployment rate. The unemployment rate is ordered second and it is allowed to adjust within the month to shocks to real activity, but not to shocks to financial conditions. This follows the standard Okun's law, which relates real activity and the labour market. Finally, shocks to real activity are ordered first and are assumed to impact the labour and financial markets after one month.

To capture changes over time in the size of the shocks, the log-volatilities are assumed to be independent stochastic processes which evolve over time according:

$$log(h_{i,t}) = log(h_{i,t-1}) + \eta_{i,t} \qquad \eta_{i,t} \sim \mathcal{N}(0, \sigma_{i,\eta}^2) \tag{4}$$

7. It is worth to mention that as discussed in Primiceri (2005) and recently outlined in Arias et al. (2021) the ordering of the variables in this model matters not only for the identification of the shocks but also for estimation. This occurs because the Normal prior on the free elements of the lower triangular matrix $\boldsymbol{A}$ induces *a priori* an asymmetric prior for the variance-covariance matrix of the reduced-form residuals.

where $i = \{PMI, \Delta U, CISS\}$ for the euro area and $i = \{CFNAI, \Delta U, NFCI\}$ for the US, and where ΔU stands for the month-on-month changes in the unemployment rate.

On the other hand, to capture changes in the symmetry of the shocks, it is assumed that the shape parameters λ_{it} are another set of independent stochastic processes with their own dynamics. In general, positive (negative) values of $\lambda_{i,t}$ are associated to right (left) skewed shocks and right (left) skewed shocks decrease the likelihood of left (right) tail events while correspondingly increase the likelihood of right (left) tail events. For example, when the shape parameters of the shocks to the unemployment rate is positive, namely $\lambda_{\Delta U,t} > 0$, the labour market shock is skewed to the right, and large increases in the unemployment rate become more likely as a consequence of this shock. We consider a specification in which the endogenous variables on real activity and financial conditions can be thought as risk factors affecting the skewness of the shocks to the unemployment rate. In intuitive terms, this implies that the monthly changes to the unemployment rate are more likely to be hit by adverse right skewed shocks when the state of the economy is weak, either via a bad performance of real activity or a strong tightening of financial conditions. In this sense, we assume that these risk factors provide information on the evolution of the shape parameter of shocks to the unemployment rate over time, following:

$$\lambda_{\Delta U,t} = \phi_{1,\Delta U} \lambda_{\Delta U,t-1} + \boldsymbol{\phi_2} \boldsymbol{x_{t-1}} + \xi_{\Delta U,t} \qquad\qquad \xi_{\Delta U,t} \sim \mathcal{N}(0, \sigma_{\xi,\Delta U}^2) \qquad (5)$$

where $\boldsymbol{x_{t-1}}$ is a vector that includes a constant and the lagged risk factors, being $\{PMI_{t-1}, CISS_{t-1}\}$ for the euro area and $\{CFNAI_{t-1}, NFCI_{t-1}\}$ for the US. This setup makes the monthly changes in the unemployment rate to be our target variable and enables to capture persistency and state dependence in the shape of the shocks to the unemployment rate in connection to past developments in real activity and in the financial conditions.[8] The coefficients in the vector $\boldsymbol{\phi_2}$ determine the relationship between the risk factors and the shape of the shocks. When this coefficient is positive, an increase in the risk factors in associated to an increase of the skewness of the shock, that is to a shift of the conditional quantiles of the change in the unemployment rate to the right; conversely, when this coefficient is negative, increases of the risk factors are associated to a decrease in the skewness of the shocks, that is, to a shift of the conditional

---

8. It is important to notice that in our specification the risk factors do not enter the variance of the shocks, thus only moving the asymmetric shape of the distribution of shocks.

quantiles of the change in the unemployment rate to the left.

In their turn, in the model, shocks to real activity and to financial conditions are allowed to be potentially asymmetric with the degree of asymmetry changing over time. In particular, we assume that the shape parameters of the shocks to the real activity and financial conditions indicators follow independent AR(1) stochastic processes

$$\lambda_{i,t} = \phi_{1,i}\lambda_{i,t-1} + \xi_{i,t} \qquad\qquad \xi_{it} \sim \mathcal{N}(0, \sigma^2_{\xi,i}) \qquad (6)$$

for $i = \{PMI, CISS\}$ in the euro area and $i = \{CFNAI, NFCI\}$ for the US.

Given that the risk factors influence not only the conditional mean of the changes in the unemployment rate through equation (1) but also the conditional skewness via equation (5), this model can capture the potential non-linear effects of real activity and financial conditions on the unemployment rate, similarly to the quantile regression framework by Kiley (2022). However our approach displays some advantages with respect to the methods based on univariate quantile regressions. First, our Bayesian VAR model allows to properly address the rich autocorrelation structure of macroeconomic time series and to exploit a potentially richer information set that is coherent over time, while this is in general more difficult in the univariate quantile regression framework. Second, we can obtain the entire predictive distribution for the changes in the unemployment rate in a single step, without the need of relying on quantile interpolation methods as it is done in the "at-risk" literature following the paper of Adrian et al. (2019). Third, we can jointly model the multivariate dynamics of all endogenous variables in our model, which in the case of our application are the changes the unemployment rate, the indicator for real activity, and the indicator for financial conditions. Quantile regression based methods focus instead on one target variable in a partial equilibrium without accounting explicitly for general equilibrium feedback effects over time. Fourth, our flexible structure allows us to assess tail risks simultaneously in multiple target variables. We will develop on this in Section 5, where we use an augmented version of our model to quantitatively assess the risk of stagflation in the euro area and in the US. Finally, a more general advantage of our BVAR methodology is that even by adding time varying skewness to the model we are still able to use all the standard tools used for policy evaluation and scenario analysis that are traditionally used in the VAR literature,

which are not readily available to univariate quantile regression based methods.[9]

3.2 Priors and estimation

The equations of the time varying skewness stochastic volatility VAR model form a non-linear and non-Gaussian state space model. The model is estimated using the Gibbs sampler algorithm described by Renzetti (2023). The estimation strategy goes around the potential difficulties arising because of non-Gaussianity of shocks by leveraging on the normal mixture representation of the skew normal distribution with a truncated normal used as the mixing distribution and by exploiting the triangularization of the VAR system as in Carriero et al. (2019) to estimate the parameters and the mixing variables equation by equation.[10] The Gibbs sampler algorithm includes particle steps to approximate the full conditional posterior distributions of the log-volatilities and the shape parameters.[11] The transition equations of the latent states are used as importance densities in the particle steps. In order to alleviate path degeneracy in the underlying conditional sequential Monte Carlo sampler, we exploit the ancestor sampling procedure that enables a fast mixing even when using seemingly few particles.[12]

As for the specification of the prior distribution for the parameters of the model, we specify a *Normal* prior for the autoregressive coefficients stored in the matrices $\boldsymbol{\Pi_j}$ with $j = 0, \ldots, p$ with Minnesota type variance covariance matrix (Litterman (1986)). Following Cogley et al. (2005), we specify a Normal prior for the free elements in the matrix $\boldsymbol{A}$. We also assume a Normal prior for the initial state of the log-volatilities $log(h_{i,0})$, for the shape parameters $\lambda_{i,0}$, for the coefficients in the state equations of the shape parameters $\phi_{1,i}$ and for the elements of $\boldsymbol{\phi_2}$. Finally, we assume an inverse Gamma prior for the variance of the innovations to the log-volatilities and for the variance of the shape parameters. Table 6 in Appendix A.3 summarises our choices on the priors and relevant hyperparameters.

9. Multivariate quantile regression based methods (as in Chavleishvili et al. (2019)) mitigate a large share of the disadvantages faced by univariate quantile regressions. The main difference between our model and a QVAR is that we use a simpler and fully parametric structure that allows us to extend the model in a more straightforward way that is also more efficient from a computational perspective.

10. See Appendix A.2 and in particular equation (13) for further details on the mixture representation.

11. It is worth to remark that in addition to referring to a multivariate model, the estimation algorithm is conceptually different from Wolf (2021) since the algorithm used in this paper leverages on the normal mixture representation of the skew normal random variable as detailed in the Appendix A.2. In particular, the estimation procedure exploits the fact that conditionally on the vector of mixing variables $\boldsymbol{v}_t$, on the elements of the diagonal matrix $\boldsymbol{\Delta_t}$ (which are one to one map to the shape parameters $\lambda_{1,t}, \ldots, \lambda_{N,t}$) and on the log-volatilities the state space is Gaussian. Further details on this difference can be found in Renzetti (2023).

12. The ancestor sampling procedure was developed by Lindsten et al. (2014), who provide a formal proof for the convergence of the algorithm and a comprehensive study on the properties of the sampler.

The steps of the Gibbs sampler to simulate draws from the joint posterior distribution of the parameters $\boldsymbol{\Theta}$, the latent states $\boldsymbol{s}$ (i.e., the log-volatilities and the shape parameters), and the mixing variables $\boldsymbol{v}$, are as follows:

1. Draw the path for the mixing variables $\{\boldsymbol{v_{it}}\}_{t=1}^T$ from $p(\boldsymbol{v_{i1}} \ldots, v_{iT}|\boldsymbol{\Theta}, \boldsymbol{s})$ for $i = 1, \ldots, N$.

2. Draw the VAR coefficients $\boldsymbol{\Pi}$ from $p(\boldsymbol{\Pi}|\boldsymbol{\Theta}, \boldsymbol{v}, \boldsymbol{s})$. The coefficients are drawn equation by equation exploiting the triangular algorithm developed in Carriero et al. (2019).

3. Draw the free elements in the lower triangular matrix $\boldsymbol{A}$ from $p(\boldsymbol{A}|\boldsymbol{\Theta}, \boldsymbol{v}, \boldsymbol{s})$.

4. Draw the variances in the state equations of the shape parameters $\sigma_{\xi,i}^2$ from $p(\sigma_{\xi,i}^2|\boldsymbol{\Theta}, \boldsymbol{s}, \boldsymbol{v})$ for $i = 1, \ldots, N$.

5. Draw the autoregressive coefficients in the state equations of the shape parameters $\phi_{1,i}$ from $p(\phi_{1,i}|\boldsymbol{\Theta}, \boldsymbol{s}, \boldsymbol{v})$ for $i = 1, \ldots, N$. and the coefficients of the risk factors in the state equation of the shape parameter of the target variable from from $p(\boldsymbol{\phi_2}|\boldsymbol{\Theta}, \boldsymbol{s}, \boldsymbol{v})$.

6. Draw the variances in the state equations of the log-volatilities $\sigma_{\eta,i}^2$ from $p(\sigma_{\eta,i}^2|\boldsymbol{\Theta}, \boldsymbol{s}, \boldsymbol{v})$ for $i = 1, \ldots, N$.

7. Draw the initial states for the volatilities $h_{i,0}$ from $p(h_{i,0}|\boldsymbol{\Theta}, \boldsymbol{v}, \boldsymbol{s})$ for $i = 1, \ldots, N$.

8. Draw the initial states for the shape parameters $\lambda_{i,0}$ from $p(\lambda_{i,0}|\boldsymbol{\Theta}, \boldsymbol{v}, \boldsymbol{s})$ for $i = 1, \ldots, N$.

9. Draw the path of the shape parameters $\{\lambda_{it}\}_{t=1}^T$ from $p(\lambda_{i1}, \ldots, \lambda_{iT}|\boldsymbol{\Theta}, \boldsymbol{v}, \boldsymbol{s})$ for $i = 1, \ldots, N$ using the particle approximation.

10. Draw the path of the volatilities $\{h_{it}\}_{t=1}^T$ from $p(h_{i1}, \ldots, h_{iT}|\boldsymbol{\Theta}, \boldsymbol{v}, \boldsymbol{s})$ for $i = 1, \ldots, N$. using the particle approximation.

The Markov Chain Monte Carlo (MCMC) algorithm consists of 50,000 draws, with the initial 30,000 draws discarded as burn-in. In the particle steps, we use 100 particles to approximate the full conditional posterior distribution of the volatilities and 150 particles to approximate the full conditional posterior distribution of the shape parameters.

4 Results

4.1 In-sample analysis

We start by examining the in-sample performance of our time varying skewness and stochastic volatility (TVSSV) VAR model. The starting point is to assess the estimated impulse response functions (IRFs) of our model. In particular, for both the euro area and the US, the IRFs identify that an expansionary shock to real activity implies a decrease in the unemployment rate, while not having a strong impact on the financial conditions. Similarly, a shock to the labour market that increases the unemployment rate has no impact on financial conditions but induces instead a feedback loop that decreases real activity. Finally, a shock that tightens the financial conditions induces a slow down in real activity and increases the unemployment rate. The IRFs unveil that the model is able to capture important relationships such as the Okun's law, in which improvements in real activity are associated with declines in the unemployment rate, and the fact that the tightening of financial conditions induces on average a slowdown in real activity and an increase in the unemployment rate.

[Figure 7 about here.]

[Figure 8 about here.]

The matrices with the autoregressive coefficients in $\mathbf{\Pi}$ and the impact matrix $\mathbf{A}$ are assumed to be constant and therefore invariant with respect to the state of the economy. As well, in the model, the impulse response functions are symmetric for both positive and negative shocks. Instead, the likelihood of good and large shocks versus bad and large shocks is state dependent and changes over time as a function of real activity and financial conditions. This implies that large adverse shocks are more likely to occur during recessions, as these are periods when real activity is depressed and financial conditions are tight. We include this potential non-linearity via equation (5), which allows for past developments in real activity and financial conditions to act as risk factors affecting the shape of the unemployment rate shocks. Table 3 presents the estimated posterior median of these coefficients and their 15th-85th credible sets. For the US we report the estimates both from the model estimated using observations up to February 2020 and the full sample in which we include time fixed effects in equation (5) to account for the Covid period.[13]

---

13. The time fixed effects cover the period from March 2020 up to July 2020.

As it would be expected, the shape parameter of shocks to the unemployment rate is estimated to increase – thus leading to extreme adverse shocks becoming more likely to materialise – following weaker developments in real activity and/or tighter financial conditions, both for the euro area and for the US. This is reflected by the sign of the estimated posterior median coefficients. However, for both areas the 15th-85th credible sets for these coefficients are wide and include zero.

Shocks to the changes in the unemployment rate exhibits both time varying volatility and time varying skewness. In particular, Figure 9 and Figure 10 shows the estimated paths for the volatility and the shape parameters in the euro area and in the United States. For the euro area, the volatility of unemployment rate shocks increased gradually over time from 1999 to 2015. The same pattern occurred in the United States over the same period. The volatility of unemployment rate shocks is however more time-varying in the US over the same period than in the euro area, although this is partially due to the longer data availability. In general, the volatility of unemployment rate shocks is broadly countercyclical in both areas, usually increasing during recessions and decreasing during expansions. However, it did not move similarly across all business cycles. For example, the increase in volatility during the Global Financial crisis and Sovereign Debt crisis were quite limited in the euro area. For the United States, the volatility of the unemployment rate shocks did not increase during the recessions in the early 1980s and increased instead right after the start of the economic recovery. Both areas recorded a strong increase in the volatility of unemployment rate shocks during the COVID pandemic. This strong increase in the unemployment rate shocks volatility was considerably more pronounced for the United States, reaching historical magnitudes as the unemployment rate suddenly increased from 3.5% in February 2020 to 14.7% in April 2020. In the euro area the volatility of unemployment rate shocks also increased but the magnitudes remained moderate, as European countries benefited from the widespread use of job retention schemes, which protected employment relations between firms and employees during the pandemic.

Shocks to the unemployment rate are on average right skewed both in the euro area and the

United States. However, the shape parameter ruling the skewness of unemployment rate shocks moves countercyclically over time and increases during recessions. This is partially explained by the cyclicality of risk factors as recessions are characterised by a lower performance of real activity and by a tightening of financial conditions.

4.2   Labour at risk

The positive skewness of unemployment rate shocks in our VAR model implies that the unemployment rate is more likely to increase at a faster pace when real activity is weaker or when financial conditions are tighter. These "bad" states of the world increase the likelihood of adverse shocks to the unemployment rate to occur. For policymakers this raises two important questions – how many jobs can be at risk in case the economy is suddenly hit by a series of large adverse shocks? And how likely is this to happen over the next year?

We define "labour-at-risk" (LaR) to be the lowest predicted increase in the unemployment rate following a series of shocks, after excluding all the more favourable outcomes that could occur at a given joint probability level. We denote this probability level to be α. Moreover, we estimate our measure of labour-at-risk for a given h-periods ahead horizon. This is,

$$LaR(\alpha)_{t+h} = F^{-1}_{\Delta^h U_{t+h}}(\alpha) \qquad \alpha \in (0,1) \qquad (7)$$

Where F^{-1} is the inverse predictive cdf of the change in the unemployment rate. In simple terms, we define labour-at-risk (α) to be the α percentile of the predictive distribution of changes in the unemployment rate h-periods ahead $(\Delta^h U_{t+h})$. We follow Kiley (2022) and focus on $\alpha = 0.8$, that is, we look to the minimum increase in the unemployment rate that would occur in case the economy was hit by shocks in the set of the 20% most adverse shocks to real activity, labour market, and financial conditions. Figure 11 for the euro area and Figure 12 for the United States show the one month ahead predictive densities for the changes in the unemployment rate in our model. For the euro area, we compute the predictive distribution of changes in the unemployment rate from January 2007 to September 2022. For the United States, we take advantage of the longer time series available and plot the predictive distribution of changes in the unemployment rate from January 1999 to September 2022. In red, we highlight the possible changes in the unemployment rate that would be equal or higher than our labour-at-risk measure at the 80th percentile.

[Figure 11 about here.]

[Figure 12 about here.]

As the Figure shows, the predictive distribution of the changes in the unemployment rate changes over time reflecting any shift in its conditional mean, in its conditional variance in its conditional skewness. Hence, shifts in the conditional mean, in the conditional variance and in the conditional skewness contribute jointly to the determine the time variation of our labour-at-risk measure. Figure 13 and Figure 14 show the estimated labour-at-risk for the euro area and the United States in a two-dimensional setup. Instead of focusing only on the predicted labour-at-risk one month ahead, we look also at different forecast horizons, and in particular we highlight the predicted labour-at-risk both one quarter ahead and one year ahead. We compare our estimates of labour at risk with those that would arise from the two-step approach from Adrian et al. (2019) that is based on quantile regressions, together with the realised value for the corresponding change in the unemployment in the same period and within the same horizon. The two econometric approaches provide observationally similar estimates for labour-at-risk.

[Figure 13 about here.]

[Figure 14 about here.]

Our labour-at-risk measure targets well on average the realised changes in the unemployment rate during recessions in both the euro area and the United States. These are periods characterised by sudden increases in the unemployment rate, implying that our labour-at-risk measure provides information on the amount of jobs that are at risk in case the economy is hit by recessionary shocks. The temporary layoffs following the COVID pandemic and the associated lockdowns in the United States provided a unique set of shocks that our labour at risk measure was not able to fully cater for. Hence, the increase in the unemployment rate in the early 2020 was an outlier considerably stronger than predicted by our labour at risk measure. For the euro area the decrease in real activity and increase in financial tightening were good predictors of the increase in the unemployment rate over the same period as the amount of temporary layoffs was limited via the widespread use of job retention schemes, which mitigated strongly possible increases in the unemployment rate. Hence, for the euro area, the increases in the unemployment rate during the COVID pandemic were considerably closer to our labour-at-risk estimate.

By contrast, our measure of labour-at-risk is higher than the changes in the unemployment rate during recoveries and expansions, as the unemployment rate usually decreases in those periods.

Relatedly, we use our model to estimate the conditional probability of "large" changes in the unemployment rate given the other variables in the model. At any given horizon h-months ahead we compute the probability of changes in the unemployment rate to be larger than a given threshold. This is calculated by computing the ratio between the number of simulated posterior draws in which changes in the unemployment rate exceed the threshold of interest, over the total number of simulated posterior draws. To identify the threshold across the different horizon, we look to the unconditional distribution of monthly, quarterly and yearly changes in the unemployment rate for both the euro area and the US. We denote large swings in the unemployment rate at the 20th percentile (i.e., a large downward swing) and 80th percentile (i.e., a large upward swing) in this distribution.[14]

[Figure 15 about here.]

[Figure 16 about here.]

Figure 15 show these probabilities for the euro area and Figure 16 for the United States. For the euro area, the periods in which the predicted probability of a quarterly change in the unemployment rate is higher coincide with the three recessions observed during our sample, in which real activity plunged and financial conditions tightened substantially.[15] Outside these recessionary periods, the model predicts only low probabilities of large increases in the unemployment rate for the euro area at 20% or below. More recently, the probability of a large yearly upward swing in the unemployment rate in the euro area increased during 2022, reaching almost 40% in September 2022 (the last observation in our sample). Conversely, the probability of large downward swings in the unemployment rate is higher during the expansionary periods and practically null during recessions. Similar results are obtained for the United States, although

14. For the euro area, large upward swings are identified when the increase in the unemployment rate is larger than 0.05 percentage points for $h = 1$ (one month ahead), 0.13pp for $h = 3$ (one quarter ahead), and 0.51pp for $h = 12$ (one year ahead). Conversely, large downward swings for the euro area are identified for decreases in the unemployment rate stronger than -0.08pp for $h = 1$, -0.23pp for $h = 3$, and -0.84pp for $h = 12$. For the US, large upward swings are identified for increases in the unemployment rate larger than 0.13pp for $h = 1$, 0.20pp for $h = 3$, and 0.83pp for $h = 12$, while large downward swings for decreases in the unemployment rate stronger than -0.15pp for $h = 1$, -0.28pp for $h = 3$, and -0.81pp for $h = 12$. Details on the percentiles of the unconditional distribution can be found in Table 7.

15. We focus on the quarterly probabilities for two reasons. First, the monthly thresholds are relatively low and more prone to short-term corrections. Second, the predicted yearly increases in the unemployment rate have larger uncertainty bands and are usually less timely for policymakers.

the probabilities of large swings in the unemployment rate are more symmetric during expansion periods than for the euro area. The post-pandemic period in the US was characterised by an increase in both the probabilities of large upward swings and large downward swings in the unemployment rate, as a result of the strong increase in the volatility of the changes in the unemployment rate that stemmed from the large reallocation flows that followed the temporary layoffs and Great Resignation, and the re-entry of these workers back into the US labour market.

4.3 Out-of-sample forecast accuracy

To assess the forecast accuracy of our model, we compare the forecasts from our time varying skewness VAR model with stochastic volatility (BVAR-TVSSV) to the forecasts from other competing models: (i) a Bayesian VAR model with *Independent Normal Inverse-Wishart* prior (BVAR), (ii) a Bayesian VAR model with stochastic volatility (BVAR-SV), and (iii) the quantile regression based method proposed by Adrian et al. (2019). This set of competing models allows us to assess the relative importance of accounting for modelling different features such as stochastic volatility, time varying skewness, and non-linearities among the risk factors and the target variables. On the one hand, the BVAR-SV, BVAR-TVSSV and quantile regression allow to capture time varying conditional volatility, while the simple BVAR cannot. On the other hand, only the BVAR-TVSSV and the quantile regression based method allow to account for time varying conditional skewness and the for the potential nonlinear effect of the real activity and financial risk factors on the labour market.[16]

The forecasting exercise is designed such that we compute the recursive one month, one quarter, and one year ahead forecasts on starting in January 2007 for the euro area and in January 1999 for the US. The forecast accuracy is evaluated using an expanding window over the sample between January 2007 and September 2022 for the euro area, described in Table 4, and over the sample between January 1999 and September 2022 for the United States, showcased in Table 5. We highlight the best performer according to various metrics in bold. These metrics comprise the average Root Mean Squared Error (RMSE) to evaluate point forecast accuracy, the average Cumulative Ranked Probability Scores (CRPS) to evaluate overall density forecast accuracy, the average right and left tail CRPS (Gneiting et al. 2011) to evaluate density forecast accuracy on the tails of the predictive distributions, and the average quantile scores at the 5th,

16. Details on the competing models are presented in the Appendix A.4.

10th, 20th, 80th, 90th, and 95th percentiles to evaluate the accuracy for targeted percentiles.[17]

[Table 4 about here.]

[Table 5 about here.]

Our BVAR TVSSV model is almost always the best performer both for euro area and for the US in terms of density forecast accuracy, as measured by the CRPS. When it is not the best model, it nevertheless provides accurate and a competing forecasts to the other models. Both quantile regression based model and our BVAR TVSSV model provide the most accurate forecasts according to the RMSE for the euro area, suggesting the importance of accounting for the non-linear effects of real activity and financial conditions on the unemployment. For the US, BVAR TVSSV and BVAR SV provide most accurate point forecasts. For what concerns density forecast accuracy, for both areas we find that our BVAR TVSSV model and the BVAR-SV often provide the most accurate density forecasts out of sample, outperforming both the simple BVAR and the quantile regression based model. This result confirms the importance of modelling changes in the conditional variance in order to obtain accurate density forecasts of the unemployment rate, consistently with Carriero et al. (2020a, 2020b). Regarding the density forecast accuracy on the tails, the best performers are often the BVAR TVSSV for the left tail and the quantile regression based model for the right tail according both to the tail weighted CRPS and the quantile scores metrics.

As a caveat, the performance of our model is sometimes not as good as that of quantile regression based methods on the right tail, while it is always outperforming quantile regression on the left tail. This comes from the fact that the median estimate of the shape parameter of the shocks to changes in the unemployment rate is estimated to be persistently positive for all the sample in analysis. That is, the model at times efficiently assigns low probability to large decreases in the unemployment rate while assigning sometimes too high probability to large increases. This comes from the flexible but parametric nature of our model which allows the shape of the distribution of shocks to vary over time according to a persistent stochastic process. This feature allows for the model structure to be easily augmented to extend the analysis towards a multivariate setting, which we will explore in the next section where we assess the risk of stagflation.

17. The details about the forecasts metrics can be found in the Appendix A.5

5 Stagflation risk

The recent sudden increase in inflation rates in both the euro area and the United States gave rise to a discussion on whether these economies would enter into a stagflation period. The term was initially coined by the British politician Iain Macleod in 1965, and was later used to assess the macroeconomic situation in the United States in the early 1970s. Stagflation is loosely defined as periods of low or negative output growth, an increasing or persistently high level of unemployment, and an inflation rate that is high by historical standards (Ha et al. (2022)).

To account for the risk of stagflation, we extend our model to include monthly data on inflation rates. For the euro area we use the Harmonized Index of Consumer Prices (HICP) for all items and for the United States we use the Consumer Price Index (CPI) for all items.[18] We slightly adjust our BVAR TVSSV to account for the year-on-year changes in the unemployment rate and the yearly inflation rate, π_t. We denote $\boldsymbol{y}_t = [\mathrm{PMI}_t, \Delta^{12}U_t, \pi_t, \mathrm{CISS}_t]$ for the euro area and $\boldsymbol{y}_t = [\mathrm{CFNAI}_t, \Delta^{12}U_t, \pi_t, \mathrm{NFCI}_t]$ for the United States, where $\Delta^h U_t = U_t - U_{t-h}$. The risk factors are left unaltered compared to the model in Section 3, but are now allowed to affect the shape of the shocks both to changes in the unemployment rate and to inflation,

$$\lambda_{\Delta^{12}U,t} = \phi_1 \lambda_{\Delta^{12}U,t-1} + \boldsymbol{\phi_2}\boldsymbol{x_{t-1}} + \xi_{\Delta^{12}U,t} \qquad \xi_{\Delta^{12}U,t} \sim \mathcal{N}(0, \sigma^2_{\xi,\Delta^{12}U})$$

$$\lambda_{\pi,t} = \rho_1 \lambda_{\pi,t-1} + \boldsymbol{\rho_2}\boldsymbol{x_{t-1}} + \xi_{\pi,t} \qquad \xi_{\pi,t} \sim \mathcal{N}(0, \sigma^2_{\xi,\pi})$$

where $\boldsymbol{x_{t-1}}$ is the vector of lagged real activity and financial risk factors. This specification is in line with López-Salido et al. (2020), who document a nonlinear relation between financial conditions and inflation using quantile regression and a Markov switching model.

We define stagflation risk as the joint probability that the yearly changes in the unemployment rate and inflation rates are above their given thresholds at any given point in time. In this way, we consider as stagflation periods those with a large increase in the unemployment rate over a year and with high inflation levels. These thresholds are identified by making use of the information in the unconditional distribution of yearly changes in the unemployment rate and inflation rates for both the euro area and the United States over time. We use the wider sample

---

18. The series for the HICP can be obtained from the ECB Statistical Data Warehouse and the series for the CPI is obtained from the FRED-MD database with the code CPIAUSL.

for the United States to calibrate our threshold for inflation.[19]

The Great Moderation brought along a period with lower turbulence to inflation (Davis et al. (2008)). This was a structural change to the economy not only driven by a decline in the volatility of the shocks, but also by the change in the way these shocks propagate (Cogley et al. (2005); Primiceri (2005); Giannone et al. (2008)). Therefore, we calibrate our thresholds for inflation and the unemployment rate changes with data from 1984 onwards for the US. The 80th percentile of the distribution of US inflation rates stands at 4%. For the yearly changes in the unemployment rate, we set the threshold at 0.5 percentage points. This corresponds to the 80th percentile for the euro area since 1999 and to the 83rd percentile for the US since 1984.

We assess the risks of stagflation in Figure 17 for the euro area. In particular, we show the estimated three months ahead joint probabilities on yearly changes in the unemployment rate exceeding the 0.5 percentage points and inflation surpassing 4%. We decompose the stagflation risk by displaying separately the labour at risk channel (in red) and the inflation risk channel (in blue).[20] The models are estimated with data available up to September 2022, implying that we assess the risk of stagflation up to December 2022.

[Figure 17 about here.]

There was only a limited risk of stagflation in the euro area since 2007. The probability of stagflation reached around 10% in December 2008 during the Global Financial crisis, first with an increase in inflation risk and later with a strong increase in the amount of labour at risk. During the Sovereign Debt crisis there was a high degree of labour at risk but no inflation risk. The risk of stagflation decreased and remained virtually null until the second half of 2022, when it started increasing driven by the persistently high levels of inflation and a gradually increasing degree of labour at risk in the economy.

Figure 18 provides further information on the risk of stagflation by contrasting the contour plots for the 20th, 50th, 80th and 90th percentiles of the bivariate predictive densities for inflation and yearly changes in the unemployment rate in the euro area between December 2008, using

---

19. The correlation between the inflation rates in the euro area and in the US stands at above 85% between January 1999 and September 2022, and inflation rates moving in a broadly synchronised way for both areas. Hence, we use the historical distribution of inflation rates in the US as an approximation for the historical distribution of inflation rates in the euro area.

20. We compute the joint probability of two variables exceeding a given threshold at a given horizon h by computing the ratio between the number of draws in which the two variables exceed the threshold over the total number of draws.

data up to September 2008, and December 2022 using data up to September 2022. While the stagflation risk reached similar magnitudes in both periods, it was closer to both borders of the stagflation area in 2008, with a more limited inflation risk and a slightly higher labour at risk. By contrast, there is a higher uncertainty in the estimate of stagflation risk in 2022 as the volatility of the bivariate predictive density is wider. This implies that it is possible for the stagflation risk to increase at a fast pace in the near future in case the degree of labour at risk is not promptly contained, given the steep response of the unemployment rate to a slower growth in real activity or to a tightening of financial conditions.

[Figure 18 about here.]

While stagflation risk remained limited for the euro area, this was not the case for the United States since 1999. In fact, our estimated measure for stagflation risk increased above 90% in the second half of 2008 and around 40% in 2010. The degree of labour at risk is highest either during or immediately after each recession, while inflation risk was consistently higher for the US before the Global Financial Crisis. We highlight the predicted increase in the stagflation risk for the US with the increase in energy prices in 2021, which preceded the developments in the euro area. However, the risk of stagflation has decreased in 2022 due to the strong performance of the US labour market, which points in our model to a lower risk of unemployment while the inflation risk remains extremely elevated.

[Figure 19 about here.]

[Figure 20 about here.]

A comparison between the estimated stagflation risk for October 2008, using data up to July 2008, and December 2022 using data up to September 2022 is showcased in Figure 20. It unveils that the current economic juncture is considerably more uncertain than that in 2008, similarly to what happened for the euro area. However, and in contrast to what was observed for the euro area, this uncertainty seems to be more prevalent in the predicted degree of labour at risk.

6 Conclusion

We develop a BVAR model with time varying skewness and stochastic volatility that caters for the fact that the unemployment rate changes are asymmetric over the business cycles, declining

slowly and on average during economic expansions and rising suddenly and violently during downturns. The model is applied to both the euro area and the United States to capture and quantify the degree of labour-at-risk in the economy, providing policymakers with timely information about possible risks affecting the labour market and showing how much can the unemployment rate increase at any given moment in time if the economy is hit by a persistent series of negative shocks. Movements in the average response of the unemployment rate and in the asymmetry of labour market shocks depend both on the developments in real activity or on the tightening of financial conditions. Further, we use our BVAR to track stagflation risk in the economy, defined as the joint event of both a high degree of labour at risk and a high inflation risk. The analysis of joint risks could prove important for the assessment of the unemployment-inflation trade-off and of the scope of monetary policy. Our work provides also the foundation for embedding asymmetric shocks as part of the toolkit used for the estimation of medium-scale DSGE models.

References

Abbritti, Mirko, and Stephan Fahr. 2013. "Downward Wage Rigidity and Business Cycle Asymmetries." *Journal of Monetary Economics* 60 (7): 871–886.

Adrian, Tobias, Nina Boyarchenko, and Domenico Giannone. 2019. "Vulnerable Growth." *American Economic Review* 109, no. 4 (April): 1263–89.

Andolfatto, David. 1997. "Evidence and Theory on the Cyclical Asymmetry in Unemployment Rate Fluctuations." *Canadian Journal of Economics* 30 (3): 709–721.

Arias, Jonas E., Juan F. Rubio-Ramirez, and Minchul Shin. 2021. *Macroeconomic Forecasting and Variable Ordering in Multivariate Stochastic Volatility Models.* Working Papers 21-21. Federal Reserve Bank of Philadelphia, June.

Azzalini, Adelchi. 1986. "Further results on a class of distributions which includes the normal ones." *Statistica* 46 (2): 199–208.

Bai, Jushan, and Serena Ng. 2005. "Tests for Skewness, Kurtosis, and Normality for Time Series Data." *Journal of Business Economic Statistics* 23:49–60.

Brownlees, Christian, and André B.M. Souza. 2021. "Backtesting global Growth-at-Risk." *Journal of Monetary Economics* 118:312–330.

Carriero, Andrea, Todd E Clark, and Massimiliano Marcellino. 2019. "Large Bayesian vector autoregressions with stochastic volatility and non-conjugate priors." *Journal of Econometrics* 212 (1): 137–154.

———. 2020a. *Capturing Macroeconomic Tail Risks with Bayesian Vector Autoregressions.* Working Papers 20-02R. Federal Reserve Bank of Cleveland, January.

———. 2020b. *Nowcasting Tail Risks to Economic Activity with Many Indicators.* Working Papers 20-13R2. Federal Reserve Bank of Cleveland, May.

Chavleishvili, Sulkhan, and Simone Manganelli. 2019. *Forecasting and stress testing with quantile vector autoregression.* Working Paper Series 2330. European Central Bank.

Cogley, Timothy, and Thomas J. Sargent. 2005. "Drifts and volatilities: monetary policies and outcomes in the post WWII US." Monetary Policy and Learning, *Review of Economic Dynamics* 8 (2): 262–302.

Davis, Steven J., and James A. Kahn. 2008. "Interpreting the Great Moderation: Changes in the Volatility of Economic Activity at the Macro and Micro Levels." *Journal of Economic Perspectives* 22:155–180.

Delle Monache, Davide, Andrea De Polis, and Ivan Petrella. 2021. *Modeling and forecasting macroeconomic downside risk.* Temi di discussione (Economic working papers) 1324. Bank of Italy, Economic Research and International Relations Area, March.

DeLong, Brad, and Larry Summers. 1986. "Are Business Cycles Symmetrical?" In *American Business Cycle: Continuity and Change,* edited by Robert Gordon, 166–79. Chicago: University of Chigago Press.

Diamond, Peter A. 1982. "Aggregate Demand Management in Search Equilibrium." *Journal of Political Economy* 90 (5): 881–894.

Falk, B. 1986. "Further Evidence on the Asymmetric Behaviour of Economic Time Series over the Business Cycle." *Journal of Political Economy* 94:1096–1109.

Ferraro, Domenico. 2018. "The asymmetric cyclical behavior of the U.S. labor market." *Review of Economic Dynamics* 30:145–162.

Ferraro, Domenico, and Giuseppe Fiori. 2022. "Search Frictions, Labor Supply, and the Asymmetric Business Cycle." *Board of Governors of the Federal Reserve System, International Finance Discussion Papers no. 1355.*

Figueres, Juan Manuel, and Marek Jarociński. 2020. "Vulnerable growth in the euro area: Measuring the financial conditions." *Economics Letters* 191 (C).

Giannone, Domenico, Lucrezia Reichlin, and Michele Lenza. 2008. "Explaining the Great Moderation: It Is Not the Shocks." *Journal of the European Economic Association* 6:621–633.

Giglio, Stefano, Bryan Kelly, and Seth Pruitt. 2016. "Systemic risk and the macroeconomy: An empirical evaluation." *Journal of Financial Economics* 119 (3): 457–471.

Gneiting, Tilmann, and Roopesh Ranjan. 2011. "Comparing Density Forecasts Using Threshold- and Quantile-Weighted Scoring Rules." *Journal of Business Economic Statistics* 29 (3): 411–422.

Ha, Jongrim, M. Ayhan Kose, and Franziska Ohnsorge. 2022. "Global Stagflation." *CEPR Discussion Paper No. DP17381,* 1–48.

Ilut, Cosmin, Matthias Kehrig, and Martin Schneider. 2018. "Slow to Hire, Quick to Fire: Employment Dynamics with Asymmetric Responses to News." *Journal of Political Economy* 126 (5): 1785–2178.

Iseringhausen, Martin. 2023. "A time-varying skewness model for Growth-at-Risk." *International Journal of Forecasting.*

Keynes, John Maynard. 1936. *The General Theory of Employment, Interest, and Money.* Macmillan.

Kiley, Michael T. 2022. "Unemployment Risk." *Journal of Money, Credit and Banking* 54 (5): 1407–1424.

Kremer, Manfred, Marco Lo Duca, and Dániel Holló. 2012. *CISS - a composite indicator of systemic stress in the financial system.* Working Paper Series 1426. European Central Bank, March.

Lindsten, Fredrik, Michael I Jordan, and Thomas B Schon. 2014. "Particle Gibbs with ancestor sampling." *Journal of Machine Learning Research* 15:2145–2184.

Litterman, Robert. 1986. "Forecasting with Bayesian Vector Autoregressions-Five Years of Experience." *Journal of Business Economic Statistics* 4 (1): 25–38.

López-Salido, J. David, and Francesca Loria. 2020. *Inflation at Risk.* Finance and Economics Discussion Series 2020-013. Board of Governors of the Federal Reserve System (U.S.), February.

McKay, Alisdair, and Ricardo Reis. 2008. "The brevity and violence of contractions and expansions." *Journal of Monetary Economics* 55:738–751.

Mitchell, Wesley Clair. 1927. *Business Cycles: The Problem and Its Setting.* National Bureau of Economic Research.

Montes-Galdón, Carlos, and Eva Ortega. 2022. *Skewed SVARs: tracking the structural sources of macroeconomic tail risks.* Working Papers 2208. Banco de España, March.

Mortensen, Dale T. 1982. "Property Rights and Efficiency in Mating, Racing, and Related Games." *American Economic Review* 72 (5): 968–979.

Neftçi, Salih N. 1984. "Are Economic Time Series Asymmetric over the Business Cycle?" *Journal of Political Economy* 92:307–328.

Newey, Whitney K., and Kenneth D. West. 1987. "A Simple, Positive Semi-Definite, Heteroskedasticity and Autocorrelation Consistent Covariance Matrix." *Econometrica* 55 (3): 703–708.

Ordoñez, Guillermo. 2013. "The Asymmetric Effects of Financial Frictions." *Journal of Political Economy* 121 (5): 844–895.

Pissarides, Christopher A. 1985. "Short-Run Equilibrium Dynamics of Unemployment, Vacancies, and Real Wages." *American Economic Review* 75 (4): 676–690.

Plagborg-Møller, Mikkel, Lucrezia Reichlin, Giovanni Ricco, and Thomas Hasenzagl. 2020. "When is growth at risk?" *Brookings Papers on Economic Activity* 2020 (1): 167–229.

Primiceri, Giorgio E. 2005. "Time varying structural vector autoregressions and monetary policy." *The Review of Economic Studies* 72 (3): 821–852.

Renzetti, Andrea. 2023. *Modelling and Forecasting Macroeconomic Risk with Time Varying Skewness Stochastic Volatility Models.*

Wolf, Elias. 2021. "Estimating growth at risk with skewed stochastic volatility models." *Available at SSRN 4030094.*

Figure 1: MoM changes in the unemployment rate and PMI output and CISS
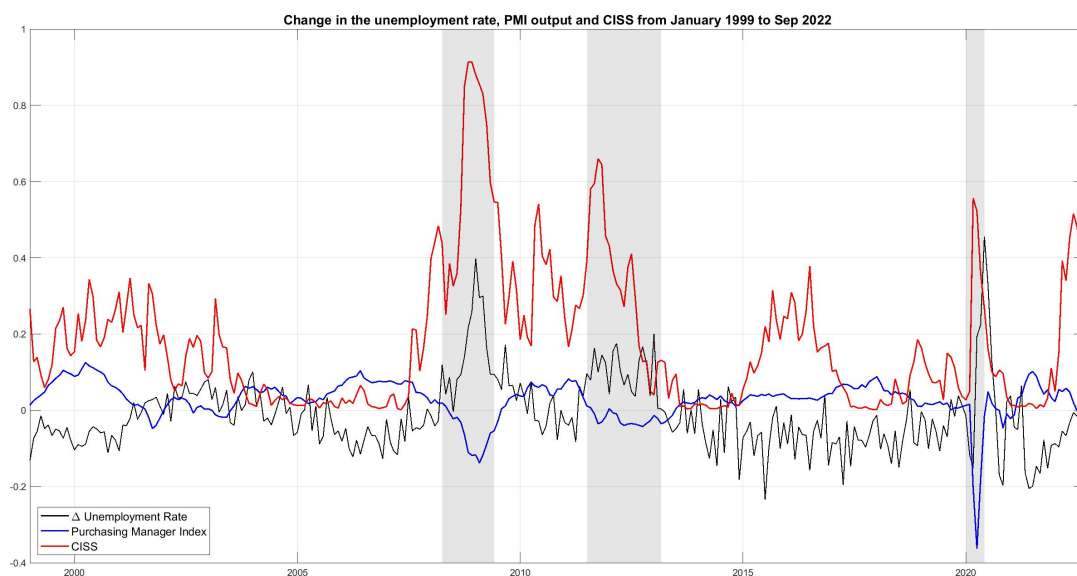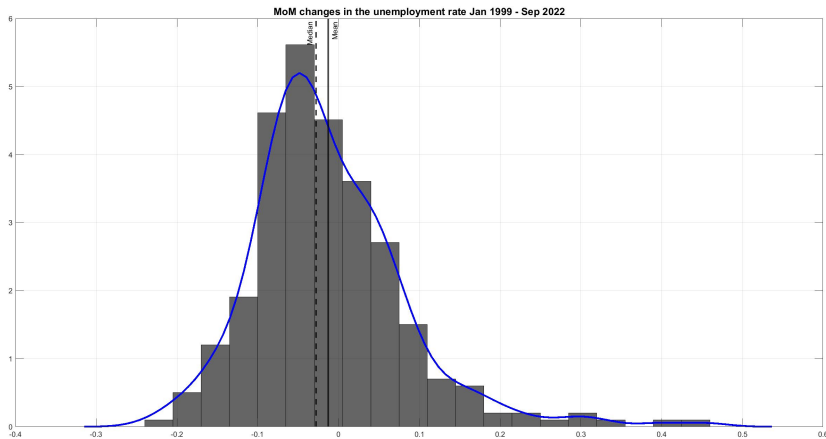

Notes: The figure shows the time series of the month-on-month changes in the unemployment rate, toghether with the PMI Output (minus 50 divided by 100) and the CISS. The shadow bands are for the EACN recessions periods.

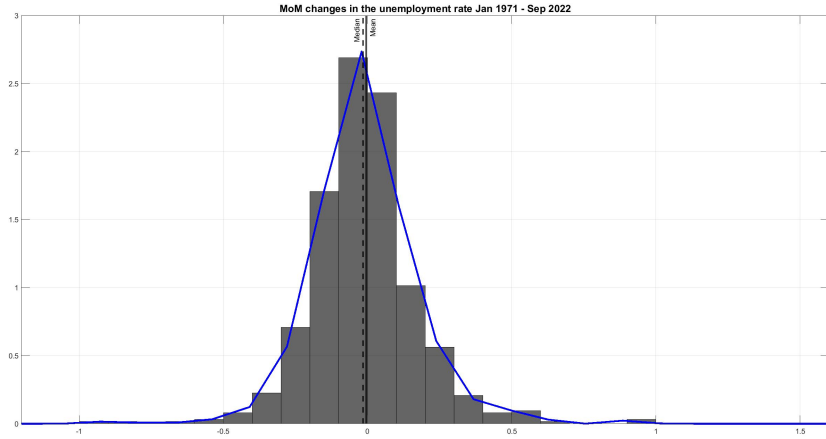## Figure 2: MoM changes in the unemployment rate and CFNAI and NFCI
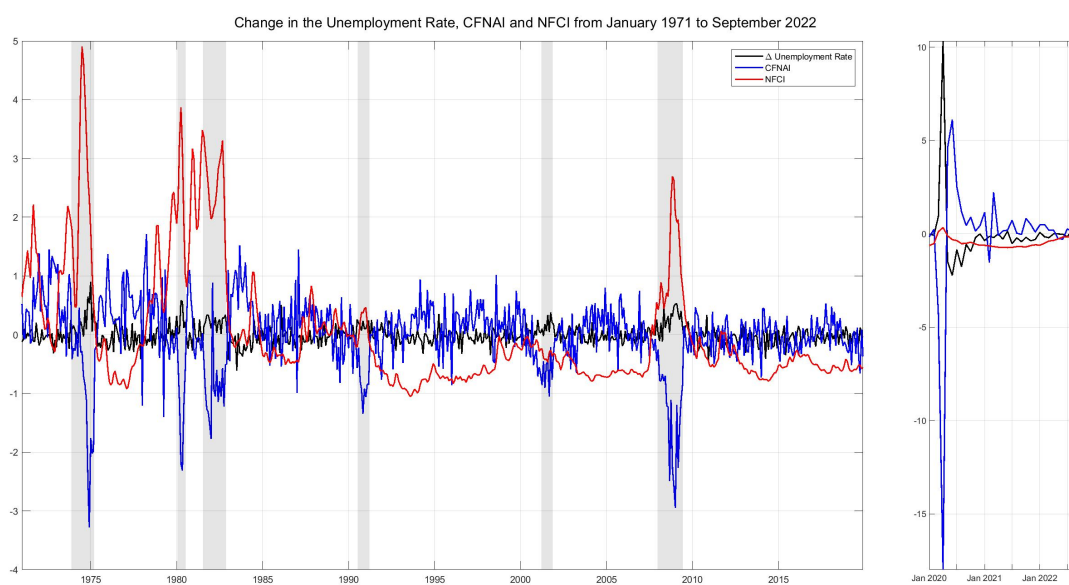
Notes: The figure shows the time series of the month-on-month changes in the unemployment rate, toghether with the CFNAI and the NFCI. The shadow bands are for the NBER recessions periods.

Figure 3: Unconditional distribution of month-on-month changes in the unemployment rate in the euro area

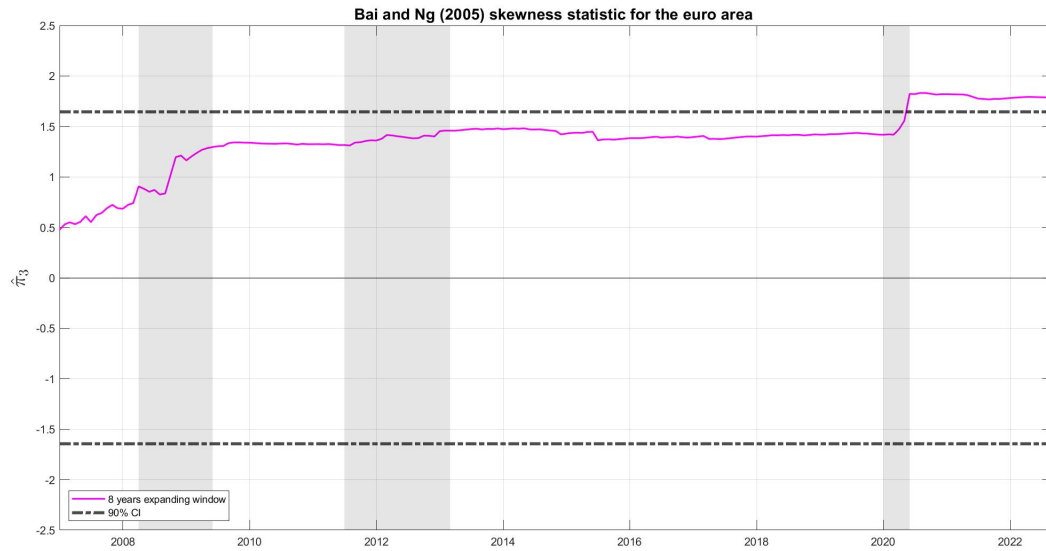**MoM changes in the unemployment rate Jan 1999 - Sep 2022**

Notes: The figure shows the histogram and the estimated distribution of the month-on-month changes in the unemployment rate from January 1999 to September 2022 in the euro area.

Figure 4: Unconditional distribution of month-on-month changes in the unemployment rate in the US
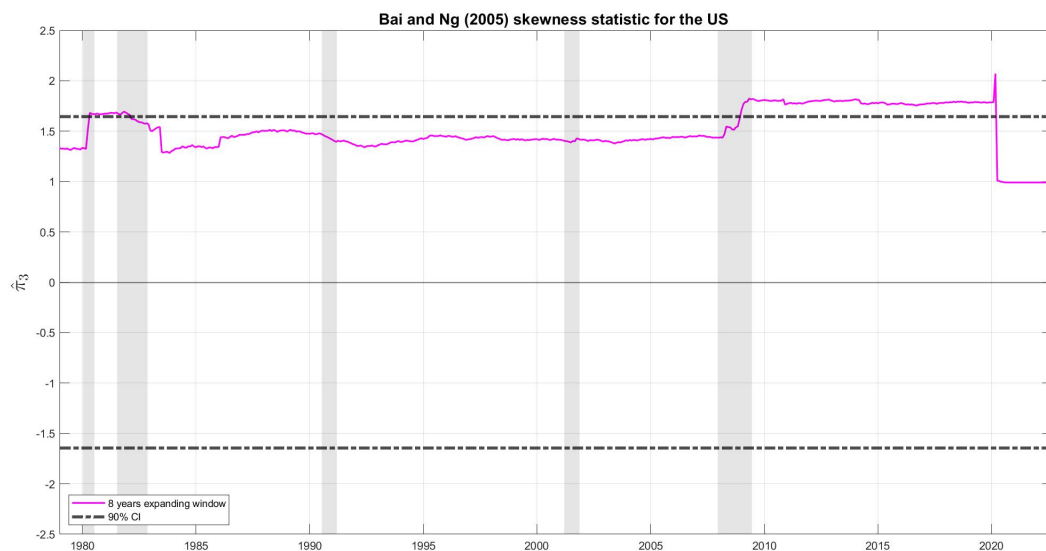

MoM changes in the unemployment rate Jan 1971 - Sep 2022

Notes: The figure shows the histogram and the estimated distribution of the month-on-month changes in the unemployment rate from January to September 2022 in the US.

Figure 5: Bai et al. (2005) skewness statistic in the euro area

**Bai and Ng (2005) skewness statistic for the euro area**

Notes: The figure shows the time series of the Bai et al. (2005) skewness statistic for the month-on-month changes in the unemployment rate in the euro area computed using expanding recursive windows of 8 years. The dashed horizontal black lines shows the 90% confidence interval.

Figure 6: Bai et al. (2005) skewness statistic in the US

**Bai and Ng (2005) skewness statistic for the US**

Notes: The figure shows the time series of the Bai et al. (2005) skewness statistic for the MoM changes in the unemployment rate in the United States computed using expanding recursive windows of 8 years. The dashed horizontal black lines shows the 90% confidence interval.

Figure 7: Estimated impulse response functions from VAR model for the euro area
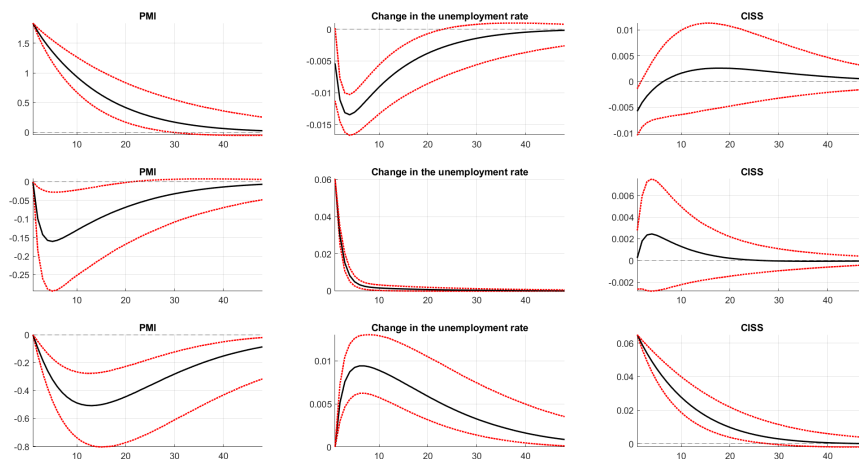

Notes: In the first row we report the impulse response functions (IRFs) to a one standard deviation shock to the real activity indicator (PMI Output). In the second row we report instead the IRFs to a one standard deviation shock to the monthly changes in the unemployment rate, and in the third row the IRFs to a one standard deviation shock to the financial conditions indicator (CISS).

Figure 8: Estimated impulse response functions from VAR model for the US
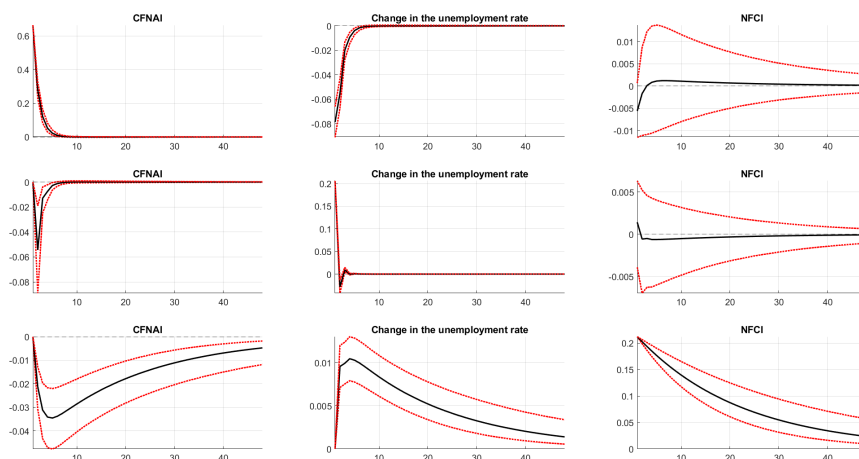
Notes: In the first row we report the impulse response functions (IRFs) to a one standard deviation shock to the real activity indicator (CFNAI). In the second row we report instead the IRFs to a one standard deviation shock to the monthly changes in the unemployment rate, and in the third row the IRFs to a one standard deviation shock to the financial conditions indicator (NFCI).

Figure 9: Estimated volatility and shape parameter of shocks to changes in the unemployment rate
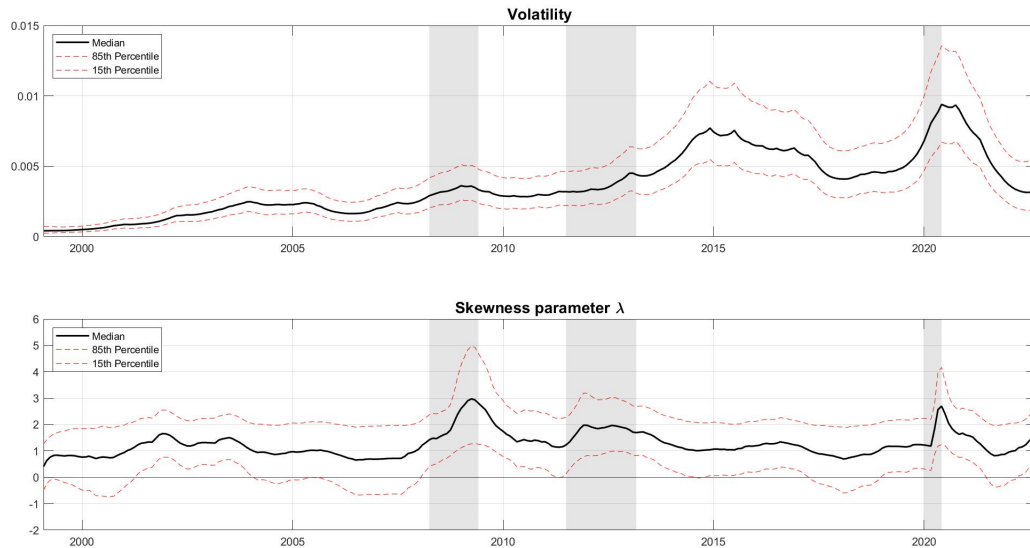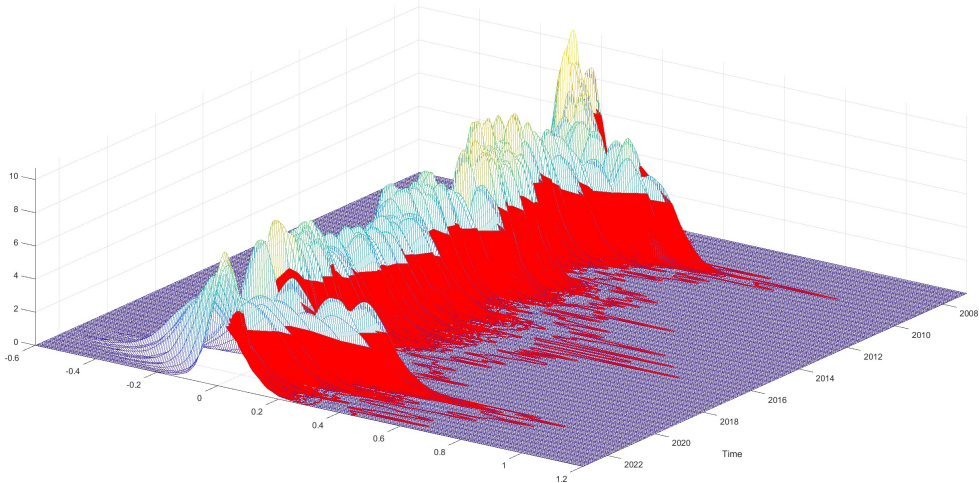

Notes: The figure shows the time series of the estimated volatilities and shape parameters of the shocks to changes in the unemployment rate in the trivariate TVSSV VAR model for the euro area. The shadow bands are for the EACN recessions periods.

Figure 10: Estimated volatility and shape parameter of shocks to changes in the unemployment rate for the US
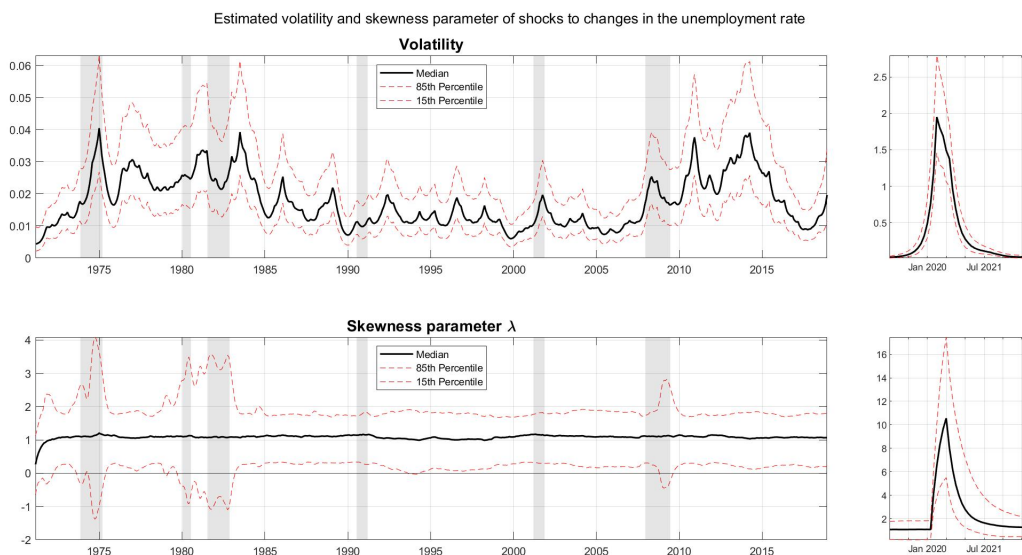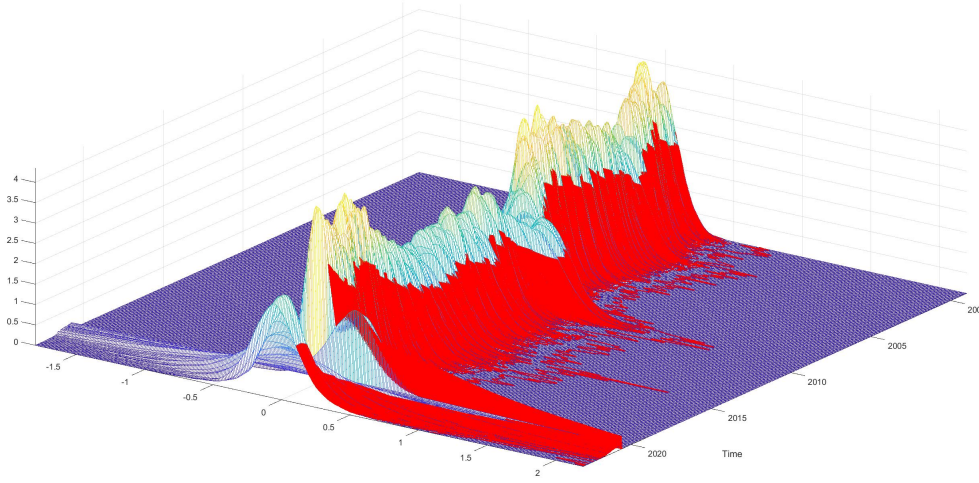

Notes: The figure shows the time series of the estimated volatilities and shape parameters of the shocks to changes in thew unemployment rate in the trivariate TVSSV VAR model for the US. The shadow bands are for the NBER recessions periods.

Figure 11: One month ahead predictive distribution of changes in the unemployment rate and 80th percentile labour-at-risk for the euro area

Notes: The figure shows the one month ahead predictive distribution for the month-on-month changes in the unemployment rate from January 2007 to September 2022 in the euro area. In red the part of the distribution on the right of the estimated 80th percentile.

Figure 12: One month ahead predictive distribution of changes in the unemployment rate and 80th percentile labour-at-risk for the US
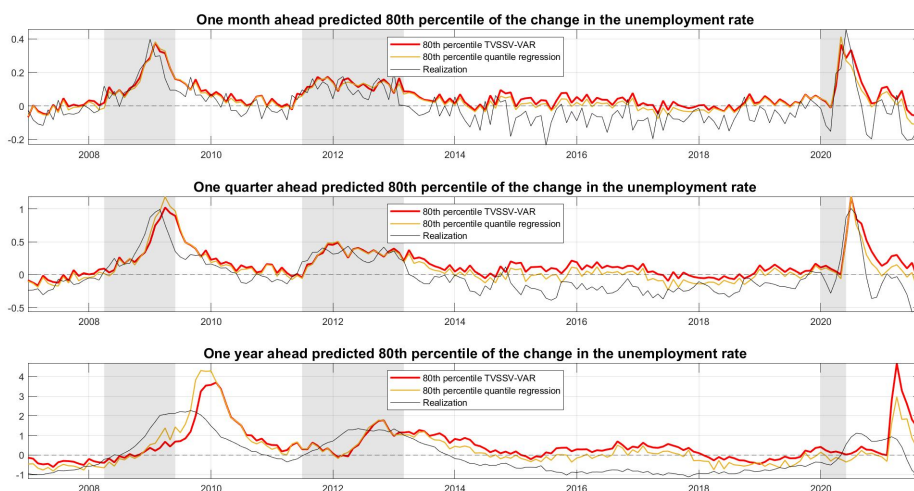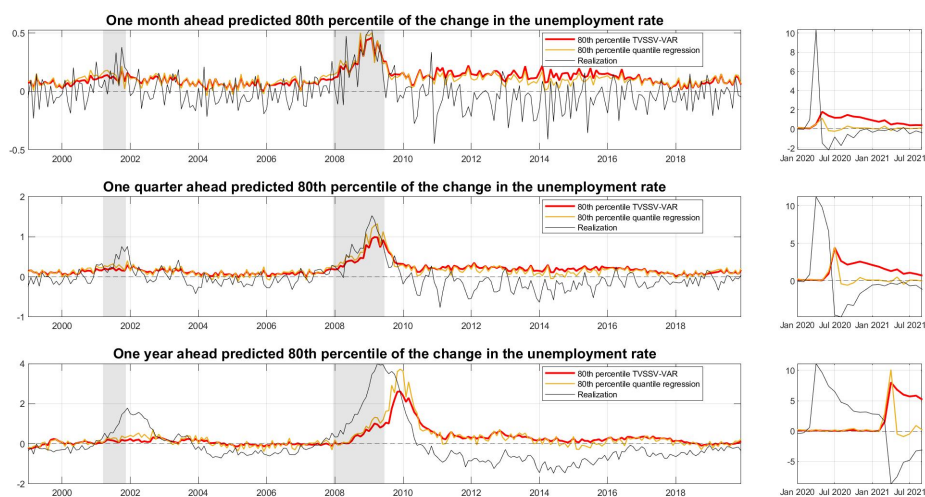

Notes: The figure shows the one month ahead predictive distribution for the month-on-month changes in the unemployment rate from January 1999 to September 2022 in the US. In red the part of the distribution on the right of the estimated 80th percentile.

Figure 13: Estimated labour-at-risk 80th percentile for the euro area

One month ahead predicted 80th percentile of the change in the unemployment rate

One quarter ahead predicted 80th percentile of the change in the unemployment rate

One year ahead predicted 80th percentile of the change in the unemployment rate

Notes: The figure shows the estimated one month ahead (first panel), one quarter ahead (second panel), and one year ahead (third panel) estimated 80th percentile of the predictive distribution of the month-on-month change in the unemployment rate (labour-at-risk) in the euro area. In red the estimates according to the TVSSV VAR model, in yellow the estimates according to the two-step quantile regression based method by Adrian et al. (2019) and in black the realization.

Figure 14: Estimated labour-at-risk 80th percentile for the US

One month ahead predicted 80th percentile of the change in the unemployment rate

One quarter ahead predicted 80th percentile of the change in the unemployment rate

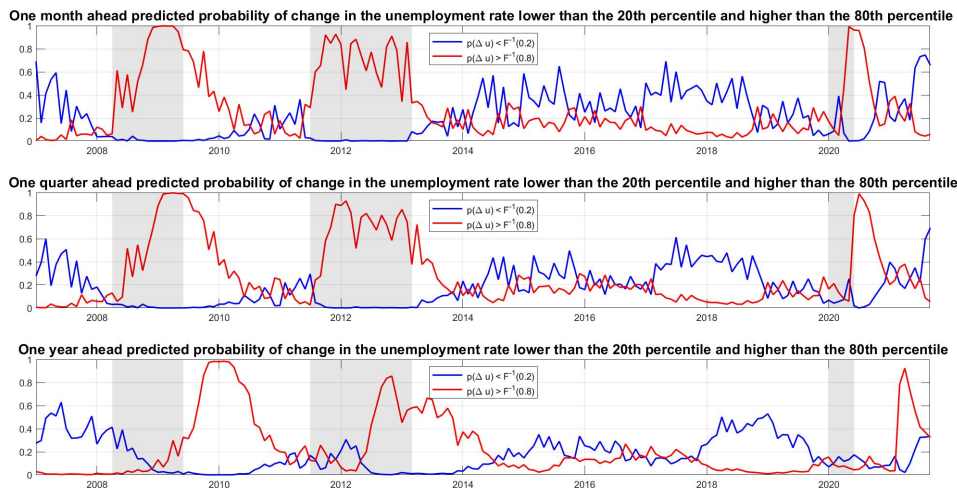**One year ahead predicted 80th percentile of the change in the unemployment rate**

Notes: The figure shows the estimated one month ahead (first panel), one quarter ahead (second panel), and one year ahead (third panel) estimated 80th percentile of the predictive distribution of the month-on-month change in the unemployment rate (labour-at-risk) in the US. In red the estimates according to the TVSSV VAR model, in yellow the estimates according to the two-step quantile regression based method by Adrian et al. (2019) and in black the realization.

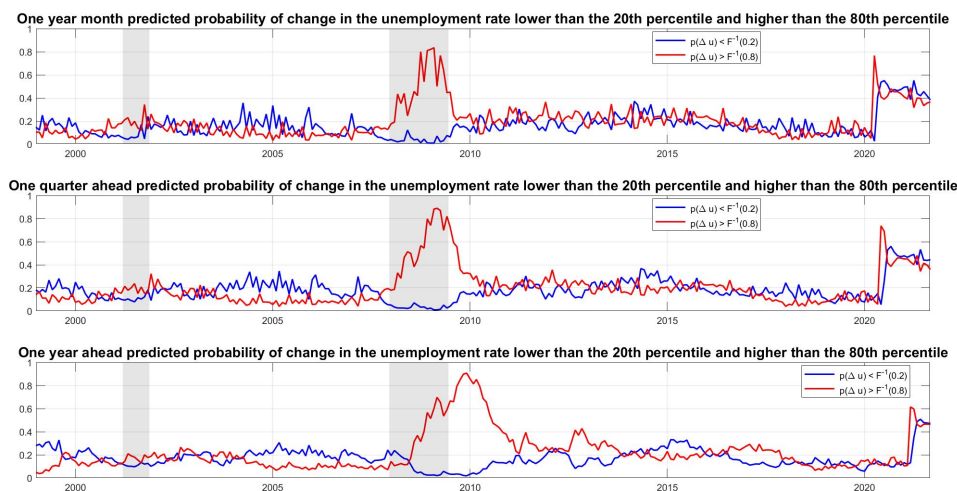Figure 15: Predicted probability of large changes in the unemployment rate for the euro area

Notes: The figure shows the estimated one month ahead (first panel), one quarter ahead (second panel), and one year ahead (third panel) probability of changes in the month-on-month change unemployment rate larger than the unconditional 20th percentile (in blue) and 80th percentile (in red) in the euro area.

Figure 16: Predicted probability of large changes in the unemployment rate for the US
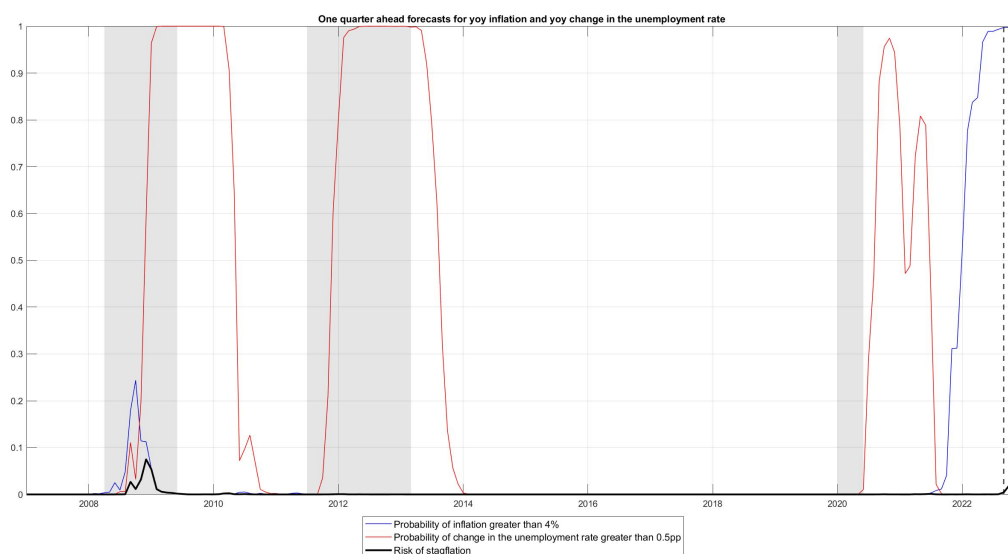

Notes: The figure shows the estimated one month ahead (first panel), one quarter ahead (second panel), and one year ahead (third panel) probability of changes in the month-on-month change unemployment rate larger than the unconditional 20th percentile (in blue) and 80th percentile (in red) in the US.

Figure 17: One quarter ahead probability of stagflation in the euro area

Notes: The figure shows the estimated one quarter ahead probability of the change in the year-on-year unemployment rate being greater than 0.5pp (in red), the year-on-year inflation rate being greater than 4% (in blue) and the probability of both events occurring (in black) in the euro area. The shadow bands are for the EACN recessions periods.

Figure 18: Contour plot for one quarter ahead joint predictive densities for π_{yoy} and ΔU_{yoy} in the euro area: December 2008 vs December 2022
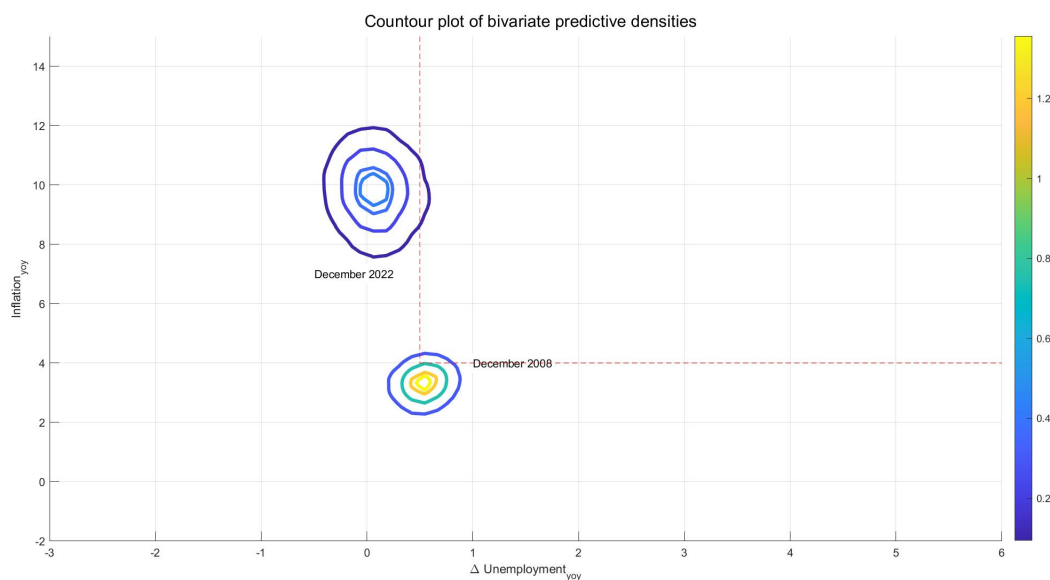
Notes: The figure shows the contours from one quarter ahead bivariate predictive density for the year-on-year change in the unemployment rate and year-on-year inflation rate for December 2008 and September 2023 in the euro area. The contours identify 20% 50%, 80% and 90% of the bivariate predictive density. The area inside the red-dotted rectangle signals year-on-year inflation greater than 4% and changes in the year-on-year unemployment rate greater than 0.5pp.

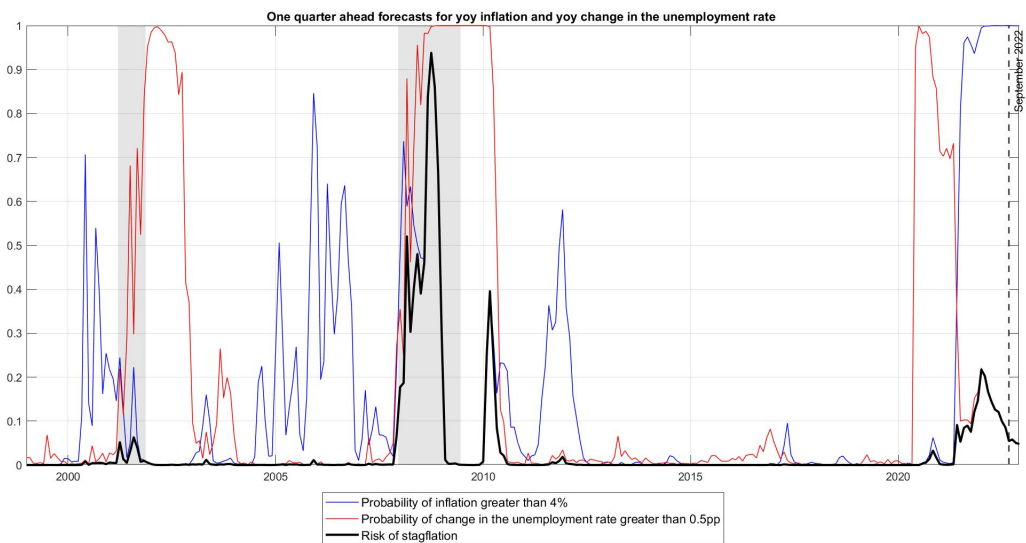Figure 19: One quarter ahead probability of stagflation in the US

Notes: The figure shows the estimated one quarter ahead probability of the change in the year-on-year unemployment rate being greater than 0.5pp (in red), the year-on-year inflation rate being greater than 4% (in blue) and the probability of both events occurring (in black) in the US. The shadow bands are for the NBER recessions periods.

Figure 20: Contour plot for one quarter ahead joint predictive densities for π_{yoy} and ΔU_{yoy} in the United States: October 2008 vs December 2022
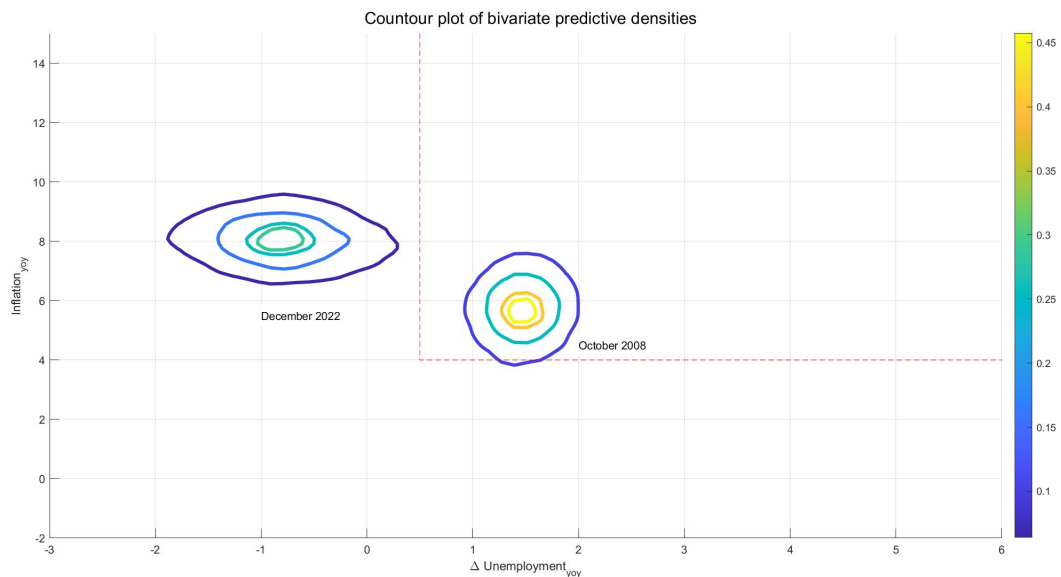

Notes: The figure shows the contours from one quarter ahead bivariate predictive density for the year-on-year change in the unemployment rate and year-on-year inflation rate for July 2009 and September 2023 in the US. The contours identify 20% 50%, 80% and 90% of the bivariate predictive density. The area inside the red-dotted rectangle signals year-on-year inflation greater than 4% and changes in the year-on-year unemployment rate greater than 0.5pp.

Table 1: Unemployment rate in the EA and the US - peak-to-trough and trough-to-peak changes

Region	Peak	Trough	Months	Peak-to-Trough (per month)	Trough	Peak	Months	Trough-to-Peak (per month)
EA					Apr-98 (*)	Mar-08	119	-0.03
	Mar-08	Jun-09	15	0.16	Jun-09	Sep-11	27	0.03
	Sep-11	Mar-13	18	0.10	Mar-13	Dec-19	81	-0.06
	Dec-19	Jun-20	6	0.09	Jun-20	Sep-22 (**)	27	-0.05
US	Nov-48	Oct-49	11	0.38	Oct-49	Jul-53	45	-0.12
	Jul-53	May-54	10	0.33	May-54	Aug-57	39	-0.05
	Aug-57	Apr-58	8	0.41	Apr-58	Apr-60	24	-0.09
	Apr-60	Feb-61	10	0.17	Feb-61	Dec-69	106	-0.03
	Dec-69	Nov-70	11	0.21	Nov-70	Nov-73	36	-0.03
	Nov-73	Mar-75	16	0.23	Mar-75	Jan-80	58	-0.04
	Jan-80	Jul-80	6	0.26	Jul-80	Jul-81	12	-0.05
	Jul-81	Nov-82	16	0.22	Nov-82	Jul-90	92	-0.06
	Jul-90	Mar-91	8	0.16	Mar-91	Mar-01	120	-0.02
	Mar-01	Nov-01	8	0.16	Nov-01	Dec-07	73	-0.01
	Dec-07	Jun-09	18	0.25	Jun-09	Feb-20	128	-0.05
	Feb-20	Apr-20	2	5.64	Apr-20	Sep-22 (**)	29	-0.39

Notes: Peaks and trough dates are taken from the CEPR for the euro area, and the months are adjusted to the end of the quarter announced by the CEPR as the relevant business cycle date, and from the NBER for the US. (*) our data for the unemployment rate in the euro area starts in April 1998. It is therefore not a trough, but our earliest comparison to the March 2008 peak. (**) our data stops for both the euro area and the US in September 2022. This is the latest comparison we have for the latest trough in each region.

Table 2: Bai et al. (2005) skewness statistic

	MoM changes	QoQ changes	YoY changes	Level
Euro Area	1.7884*	1.704*	1.5888	1.3458
US	0.9908	1.0261	1.0165	2.1551**

Notes: Bai et al. (2005) skewness statistic. * indicates rejections of the null hypothesis at 90% CI and ** indicates rejections of the null hypothesis at 95% CI.

Table 3: Coefficients in the state equation of the shape parameter λ_{Δ_u}

Euro area	$\phi_{\lambda_{t-1}}$	$\phi_{PMI_{t-1}}$	$\phi_{CISS_{t-1}}$	c_λ
	0.7314	-0.0200	0.3120	0.3669
	[0.5845 0.8526]	[−0.0438 0.0043]	[−0.3336 1.0671]	[0.7180 0.1345]
US	$\phi_{\lambda_{t-1}}$	$\phi_{CFNAI_{t-1}}$	$\phi_{NFCI_{t-1}}$	c_λ
Full sample	0.7536	-0.0061	0.0046	0.2576
	[0.5842 0.8782]	[−0.0688 0.0613]	[−0.1824 0.2110]	[0.0635 0.5155]
Pre-Covid	0.6880	-0.0230	0.0123	0.1753
	[0.5367 0.8256]	[−0.1605 0.0973]	[−0.1824 0.2110]	[−0.0116 0.4277]

Notes: The Table reports the posterior median estimates with 85th and 15th credible sets in brackets of the coefficients of the risk factor in the state equation for the shape parameters of the shocks to the change in the unemployment rate. For the US we report estimates based both on full sample and pre-Covid.

Table 4: Forecast accuracy January 2007 - September 2022 in the euro area

	RMSE	CRPS	LTw-CRPS	RTw-CRPS	QS 5th	QS 10th	QS 20th	QS 80th	QS 90th	QS 95th
a) One month ahead change										
BVAR	0.0051	0.0399	0.0117	0.0126	0.0067	0.0112	0.0176	0.0202	**0.0128**	**0.0077**
BVAR SV	0.0050	0.0396	0.0116	0.0126	**0.0064**	**0.0110**	**0.0175**	**0.0201**	0.0132	0.0081
BVAR TVSSV	**0.0049**	**0.0395**	**0.0115**	0.0126	0.0066	0.0114	0.0180	0.0212	0.0140	0.0087
Quantile regression	0.0049	0.0396	0.0120	**0.0123**	0.0084	0.0131	0.0194	0.0206	0.0137	0.0087
b) One quarter ahead change										
BVAR	0.0298	0.0964	0.0277	0.0313	0.0162	0.0266	0.0418	0.0521	0.0340	0.0200
BVAR SV	0.0285	0.0936	0.0263	0.0310	0.0150	0.0240	0.0384	0.0514	0.0347	0.0212
BVAR TVSSV	0.0276	**0.0926**	**0.0257**	0.0310	**0.0146**	**0.0238**	**0.0382**	0.0524	0.0361	0.0223
Quantile regression	**0.0270**	0.0949	0.0304	**0.0281**	0.0244	0.0361	0.0508	**0.0455**	**0.0304**	**0.0193**
c) One year ahead change										
BVAR	0.8184	0.4726	0.1300	0.1583	0.0770	0.1183	0.1948	0.2775	0.1819	**0.1078**
BVAR SV	0.5974	0.4265	0.1085	0.1538	0.0574	0.0934	0.1540	0.2735	0.1995	0.1340
BVAR TVSSV	0.5797	**0.4212**	**0.1055**	0.1538	**0.0549**	**0.0892**	**0.1469**	0.2747	0.2014	0.1375
Quantile regression	**0.5303**	0.4568	0.1488	**0.1387**	0.1521	0.1974	0.2450	**0.2238**	**0.1720**	0.1254

Notes: The Table reports the average Root Mean Squared Error (RMSE), Average Cumulative Ranked Probability Score, Average Right and Left Tail Weigthed probability score and the Quantile Scores for the 5th, 10th, 20th 80th 90th percentiles. In bold the best model according to each forecast metrics.

Table 5: Forecast accuracy January 1999 - September 2022 in the US

	RMSE	CRPS	LTw-CRPS	RTw-CRPS	QS 5th	QS 10th	QS 20th	QS 80th	QS 90th	QS 95th
a) One month ahead change										
BVAR	0.7309	0.1683	0.0520	0.0551	0.0501	0.0653	0.0817	0.0868	0.0707	0.0567
BVAR SV	0.4176	0.1355	0.0337	0.0512	0.0190	0.0306	**0.0461**	0.0835	0.0679	0.0561
BVAR TVSSV	**0.4128**	**0.1337**	**0.0333**	0.0505	**0.0185**	**0.0304**	0.0489	0.0854	0.0700	0.0581
Quantile regression	0.4240	0.1432	0.0441	**0.0468**	0.0434	0.0553	0.0699	**0.0735**	**0.0604**	**0.0509**
b) One quarter ahead change										
BVAR	3.4308	0.3669	0.1136	0.1210	0.1137	0.1452	0.1800	0.1930	0.1591	0.1295
BVAR SV	**1.2565**	**0.2819**	**0.0684**	0.1094	**0.0360**	**0.0617**	**0.0965**	0.1798	0.1521	0.1282
BVAR TVSSV	1.2572	0.2823	0.0687	**0.1091**	0.0378	0.0637	0.1010	0.1847	0.1562	0.1319
Quantile regression	1.3636	0.3004	0.0935	0.0988	0.1007	0.1229	0.1492	**0.1559**	**0.1325**	**0.1155**
c) One year ahead change										
BVAR	14.8082	0.8996	0.2562	0.3111	0.2142	0.2947	0.3965	0.5239	0.4230	0.3299
BVAR SV	**3.1297**	0.7385	0.1674	0.2989	0.0871	0.1416	0.2268	0.5108	0.4469	0.3814
BVAR TVSSV	3.1475	**0.7369**	**0.1670**	0.2979	**0.0843**	**0.1403**	**0.2233**	0.5088	0.4436	0.3782
Quantile regression	3.5671	0.7723	0.2205	**0.2694**	0.1946	0.2594	0.3469	**0.4360**	**0.3764**	**0.3216**

Notes: The Table reports the average Root Mean Squared Error (RMSE), Average Cumulative Ranked Probability Score, Average Right and Left Tail Weigthed probability score and the Quantile Scores for the 5th, 10th, 20th 80th 90th percentiles. In bold the best model according to each forecast metrics.

A   Appendix

A.1   Bai et al. (2005) test for skewness

Under the null hypothesis of no asymmetry Bai et al. (2005) test statistic is:

$$\hat{\pi}_3 = \frac{\sqrt{T}\hat{\mu}_3}{s(\hat{\mu}_3)} \xrightarrow{d} \mathcal{N}(0,1) \tag{8}$$

where $\hat{\mu}_3$ is the sample estimate of the third central moment of the distribution and $s(\hat{\mu}_3) = (\hat{\boldsymbol{\alpha}}_2 \hat{\boldsymbol{\Gamma}}_{22} \hat{\boldsymbol{\alpha}}_2')^{\frac{1}{2}}$ $\hat{\boldsymbol{\alpha}}_2 = [1, -3\hat{\sigma}^2]$. $\hat{\sigma}^2$ is a consistent estimate of the variance σ^2 and $\hat{\boldsymbol{\Gamma}}_{22}$ is a consistent estimate of the 2×2 sub-matrix of $\boldsymbol{\Gamma} = \lim_{T\to\infty} T\,\mathbb{E}[\bar{Z}\bar{Z}]$ where $\bar{Z}$ is the sample mean of $\boldsymbol{Z}_t$, defined as the deviation of the empirical centered first three moments from the Gaussian's one, namely:

$$\boldsymbol{Z_t} = \begin{bmatrix} (X_t - \mu)^3 - \mu_3 \\ (X_t - \mu) \\ (X_t - \mu)^2 - \sigma^2 \end{bmatrix}$$

The long run variance is estimated following Newey et al. (1987).

A.2   TVSSV-VAR with Skew normal shocks

The TVSSV VAR(p) model with *Skew Normal* shocks is given by:

$$\boldsymbol{y_t} = \boldsymbol{\Pi_0} + \boldsymbol{\Pi_1 y_{t-1}} + \ldots + \boldsymbol{\Pi_p y_{t-p}} + \boldsymbol{A}^{-1}\boldsymbol{H}_t^{0.5}\boldsymbol{\varepsilon_t} \tag{9}$$

$$\varepsilon_{it} \sim Skew\ normal(\zeta_{it}, \omega_{it}, \lambda_{it})$$

$$log(h_{i,t}) = log(h_{i,t-1}) + \eta_{i,t} \qquad \eta_{i,t} \sim \mathcal{N}(0, \sigma^2_{i,\eta}) \tag{10}$$

with $i = \{PMI, \Delta U, CISS\}$ for the euro area and $i = \{CFNAI, \Delta U, NFCI\}$ for the US.

$$\lambda_{\Delta U,t} = \phi_1 \lambda_{\Delta U,t-1} + \boldsymbol{\phi_2 x_{t-1}} + \xi_{\Delta U,t} \qquad \xi_{\Delta U,t} \sim \mathcal{N}(0, \sigma^2_{\xi,\Delta U}) \tag{11}$$

$$\lambda_{i,t} = \phi_1 \lambda_{i,t-1} + \xi_{i,t} \qquad \xi_{it} \sim \mathcal{N}(0, \sigma^2_{\xi,i}) \tag{12}$$

with $i = \{PMI, CISS\}$ for the euro area and $i = \{CFNAI, NFCI\}$ for the US. The *Skew normal* (Azzalini 1986) distribution is:

$$p(\varepsilon_t|\zeta, \omega^2, \lambda) = \frac{2}{\omega} \phi\left(\frac{\varepsilon_t - \zeta}{\omega}\right) \Phi\left(\lambda\left(\frac{\varepsilon_t - \zeta}{\omega}\right)\right)$$

where $\phi(.)$ and $\Phi(.)$ are respectively the probability density function and the cumulative density function of the Standard Normal. The mean and the variance of ε_t are given by $\mathbb{E}[\varepsilon_t] = \zeta + \omega\delta\sqrt{\frac{2}{\pi}}$ and $var(\varepsilon_t) = \omega^2\left(1 - \frac{2\delta^2}{\pi}\right)$. Assuming $\mathbb{E}[\varepsilon_t] = 0$ and $var(\varepsilon_t) = 1$ implies the following constraints on the location and scale parameters $\zeta = -\omega\delta\sqrt{\frac{2}{\pi}}$ and $\omega^2 = \left(1 - \frac{2\delta^2}{\pi}\right)^{-1}$.

To estimate the TVSSV model we exploit the fact that $\varepsilon_t \sim Skew - Normal(\zeta, \omega^2, \lambda)$ has the following stochastic representation:

$$\varepsilon_t = \zeta + \delta\omega v_t + \sqrt{(1 - \delta^2)}\omega z_t \tag{13}$$

where $v_t \overset{i.i.d}{\sim}$ Truncated normal$_{[0,\infty)}(0,1)$ $z_t \overset{i.i.d}{\sim} \mathcal{N}(0,1)$ and $\delta = \frac{\lambda}{\sqrt{1+\lambda^2}}$, with $-1 < \delta < 1$.

Using the stochastic representation in equation (13) for the shocks, we can write the VAR system as:

$$\boldsymbol{y_t} = \boldsymbol{\Pi_0} + \boldsymbol{\Pi_1}\boldsymbol{y_{t-1}} + \ldots + \boldsymbol{\Pi_p}\boldsymbol{y_{t-p}} + \boldsymbol{A}^{-1}\boldsymbol{H_t}^{0.5}(\boldsymbol{\zeta_t} + \boldsymbol{\Omega_t}\boldsymbol{\Delta_t}\boldsymbol{v_t} + \boldsymbol{\Omega_t}(\boldsymbol{I_n} - \boldsymbol{\Delta_t^2})^{0.5}\boldsymbol{z_t}) \tag{14}$$

where:

$\boldsymbol{\zeta_t} = [\zeta_{1,t}, \ldots, \zeta_{N,t}]'$

$\boldsymbol{\Omega_t} = diag(\omega_{1t} \ldots \omega_{Nt})$

$\boldsymbol{\Delta_t} = diag(\delta_{1t} \ldots \delta_{Nt})$

$\boldsymbol{v_t} = [v_{1,t}, \ldots, v_{N,t}]' \qquad v_{i,t} \sim TruncatedNormal_{(0,\infty)}(0,1)$

$\boldsymbol{z_t} = [z_{1,t}, \ldots, z_{N,t}]' \qquad z_{it} \sim N(0,1)$.

This representation implies that conditionally on the mixing variables in $\boldsymbol{v_t}$ the likelihood is Gaussian. This allows to resuscitate and adapt many of the closed form formulas for the full conditional posterior distributions for the parameters of the model from the standard Gaussian stochastic volatility VAR model (Carriero et al. 2019). It is worth to remark that the diagonal elements in the vector $\boldsymbol{\zeta_t}$ and in the diagonal matrix $\boldsymbol{\Omega_t}$ are neither parameters nor latent states to be estimated, and satisfy the constraints (2) and (3) so that the parameterization of the shocks is correct. The diagonal elements in $\boldsymbol{\Delta_t}$ satisfy $\delta_{it} = \frac{\lambda_{it}}{\sqrt{1+\lambda_{it}^2}}$. The elements in the diagonal matrix $\boldsymbol{H_t} = diag(h_{1t}, \ldots, h_{1N})$ and the shape parameters λ_{it} are instead latent states

satisfying the transition equations (10) (11) and (12). For details on the estimation of the model see Renzetti (2023).

A.3   Priors of the TVSSV-VAR

Table 6 presents the details on the priors for the parameters of the time varying skewness stochastic volatility model:

Table 6: Priors for the parameters of the TVSSV-VAR model

Parameter	Prior
$vec(\mathbf{\Pi})$	$\mathcal{N}(vec(\underline{\boldsymbol{\mu_\Pi}}), \underline{\boldsymbol{\omega_\Pi}})$
a_{ij}	$\mathcal{N}(0, 100)$
$\phi_{i,1}$	$\mathcal{N}(1, \theta_1)$
$\boldsymbol{\phi_2}$	$\mathcal{N}(\mu_{\boldsymbol{\phi_2}}, \Sigma_{\boldsymbol{\phi_2}})$
$log(h_{i0})$	$\mathcal{N}(h_{i0}, 100)$
λ_{i0}	$\mathcal{N}(0, 10)$
$\sigma_{i,\xi}^2$	$InverseGamma(5, 0.16)$
$\sigma_{i,\eta}^2$	$InverseGamma(5, 0.16)$

Notes: The table presents the prior distribution of the parameters of the TVSSV-VAR model.

where $\underline{\boldsymbol{\omega_\Pi}}$ has the Minnesota type (Litterman 1986) prior:

$$
v_{ij,l} = \begin{cases} \frac{\theta_1}{l^{\theta_4}} & \text{if} \quad i = j \\ \frac{\sigma_i^2 \theta_1 \theta_2}{\sigma_j^2 l^{\theta_4}} & \text{if} \quad i \neq j \end{cases} \tag{15}
$$

The elements of $vec(\underline{\boldsymbol{\mu_\Pi}})$ are equal zero for the coefficients on the cross-equation lags and equal to one for the coefficients of the own lags. As for the hyper-parameters, we set $\theta_1 = 0.04$ $\theta_2 = 0.25$ $\theta_3 = 100$ $\theta_4 = 2$. We estimate σ_i^2 from univariate AR(12) regressions. For the initial state of the volatility, the prior mean h_{i0} where $h_{i,0}$ is the estimated variance from an AR(4) model to each series using as sample the first 40 observations. For the Normal prior for the coefficients on the risk factors in the state equation for the shape parameters of the shocks to changes in the unemployment rate $\boldsymbol{\phi_2}$ we assume a mean $\underline{\mu_{\boldsymbol{\phi_2}}} = [0, \dots, 0]'$ and variance covariance matrix $\underline{\Sigma_{\boldsymbol{\phi_2}}} = diag\left(\frac{\theta_1 \theta_5}{\sigma_1^2 l^{\theta_4}}, \dots \frac{\theta_1 \theta_5}{\sigma_j^2 l^{\theta_4}}\right)$ with $\theta_5 = 0.1$.

A.4   Competing models in the forecasting exercise:

In Section 4.2 we compare the forecasts from the time varying skewness stochastic volatility VAR model to the forecasts from:

- A Bayesian VAR with *Independent Normal Inverse-Wishart* prior.

- A Bayesian VAR with stochastic volatility.

- The two step approach based on quantile regression and *Skew-t* interpolation by (Adrian et al. 2019).

A.4.1 Bayesian VAR with Independent Normal Inverse-Wishart prior

The Bayesian VAR with Independent Normal Inverse-Wishart prior is given by:

$$\boldsymbol{Y} = \boldsymbol{X}\boldsymbol{\Pi} + \boldsymbol{U} \qquad \boldsymbol{U} \sim MVN(\boldsymbol{0}, \boldsymbol{\Sigma}, \boldsymbol{I_T}) \tag{16}$$

where $\boldsymbol{Y}$ is $T \times N$, $\boldsymbol{X}$ is $T \times k$ with $k = Np+1$, $\boldsymbol{\Pi}$ is $k \times n$, $\boldsymbol{U}$ is $T \times N$ and MVN stands for the matricvariate normal. The prior for the autoregressive coefficients and the variance covariance matrix is:

$$vec(\boldsymbol{\Pi}) \sim \mathcal{N}(vec(\boldsymbol{\underline{\mu_\Pi}}), \boldsymbol{\underline{\Omega_\Pi}}) \tag{17}$$

$$\boldsymbol{\Sigma} \sim \mathcal{IW}(\boldsymbol{S_0}, v_0) \tag{18}$$

$vec(\boldsymbol{\Pi})$ and $\boldsymbol{\underline{\Omega_\Pi}}$ have the same structure in A.3, and we assume $\boldsymbol{S_0} = (T-2)diag(\sigma_1^2 \ldots, \sigma_N^2)$ where we estimate σ_i^2 from univariate AR(12) regressions $v_0 = N + 2$.

A.4.2 Bayesian VAR with stochastic volatility

The BVAR with SV is given by:

$$\boldsymbol{y_t} = \boldsymbol{\Pi_0} + \boldsymbol{\Pi_1}\boldsymbol{y_{t-1}} + \ldots + \boldsymbol{\Pi_p}\boldsymbol{y_{t-p}} + \boldsymbol{A^{-1}}\boldsymbol{H_t^{0.5}}\boldsymbol{\varepsilon_t} \tag{19}$$

$$\varepsilon_{it} \sim \mathcal{N}(0,1)$$

where $\boldsymbol{A^{-1}}$ is a lower triangular matrix with ones on the main diagonal, $\boldsymbol{H_t} = diag(h_{1,t}, \ldots, h_{i,t})$ is the diagonal matrix collecting the volatilities of the shocks and $\boldsymbol{\varepsilon_t}$ is a column vector collecting the *Normal* shocks. The log-volatilities evolve according to:

$$log(h_{i,t}) = log(h_{i,t-1}) + \eta_{i,t} \qquad \eta_{i,t} \sim \mathcal{N}(0, \sigma_{i,\eta}^2) \tag{20}$$

with $i = \{PMI, \Delta U, CISS\}$ for the euro area and $i = \{CFNAI, \Delta U, NFCI\}$. As for the prior for the free elements in $\boldsymbol{A}^{-1}$ and $vec(\boldsymbol{\Pi})$ and $\underline{\boldsymbol{\Omega_\Pi}}$, have the same structure in A.3 as well we assume the same Inverse Gamma prior for $\sigma^2_{i,\eta}$.

A.4.3 Quantile regression and Skew-t interpolation

Following Adrian et al. (2019) we adopt a two-step procedure to estimate the entire predictive distribution of changes in the unemployment rate as a function of real and financial risk factors. In the first step, we use predictive quantile regression to estimate the quantiles of the conditional distribution, namely:

$$\hat{Q}_{\Delta U_{t+h}|\mathcal{I}_t}(\tau) = \hat{\boldsymbol{\beta}}_{\mathbf{1}}^\tau \Delta U_t + \hat{\boldsymbol{\beta}}_{\mathbf{2}}^\tau realrisk_t + \hat{\boldsymbol{\beta}}_{\mathbf{3}}^\tau financialrisk_t$$

for $\quad \tau = 0.05, \ldots, 0.95$ $realrisk_t = PMI$ and $financialrisk_t = CISS$ for the euro area and $realrisk_t = CFNAI$ and $financialrisk_t = NFCI$ for the US. Then, in the second step, the estimated quantiles we interpolate using a flexible *Skew-t* distribution, so as to obtain a complete predictive density for the dependent variable.

A.5 Forecasts metrics

Defining y the realization of the series to predict, $f(.)$ the density forecast and $F(.)$ corresponding the cumulative distribution, CRPS are defined as:

$$CRPS(f,y) = \int_{-\infty}^{\infty} PS(F(z), \mathbb{1}\{y \le z\})dz = \int_0^1 QS_\alpha(F^{-1}(\alpha), y)d\alpha \tag{21}$$

where

$$PS(F(z), \mathbb{1}\{y \le z\}) = (F(z) - \mathbb{1}\{y \le z\})^2 \tag{22}$$

is the Brier probability score and

$$QS_\alpha(F^{-1}(\alpha), y) = 2(\mathbb{1}\{y \le F^{-1}(\alpha)\} - \alpha)(F^{-1}(\alpha) - y) \tag{23}$$

is the Quantile Score. The Quantile Weighted CRPS are computed as:

$$twCRPS = \int_{-\infty}^{\infty} PS(F(z), \mathbb{1}\{y \le z\})^2 w(z)dz = \int_0^1 QS_\alpha(F^{-1}(\alpha), y)v(\alpha)d\alpha \tag{24}$$

where $v(\alpha) = (1 - \alpha)^2$ assigns higher weights to the lower quantiles of the distribution function.
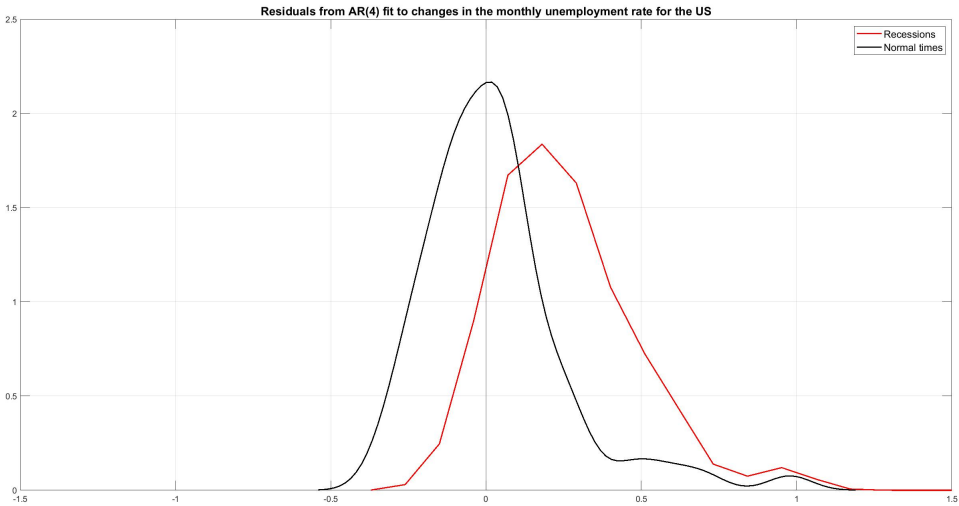
A.6 Additional figures

Figure 21: Residuals from autoregressive fit to changes in the unemployment rate in the euro area distinguishing recessions form normal times
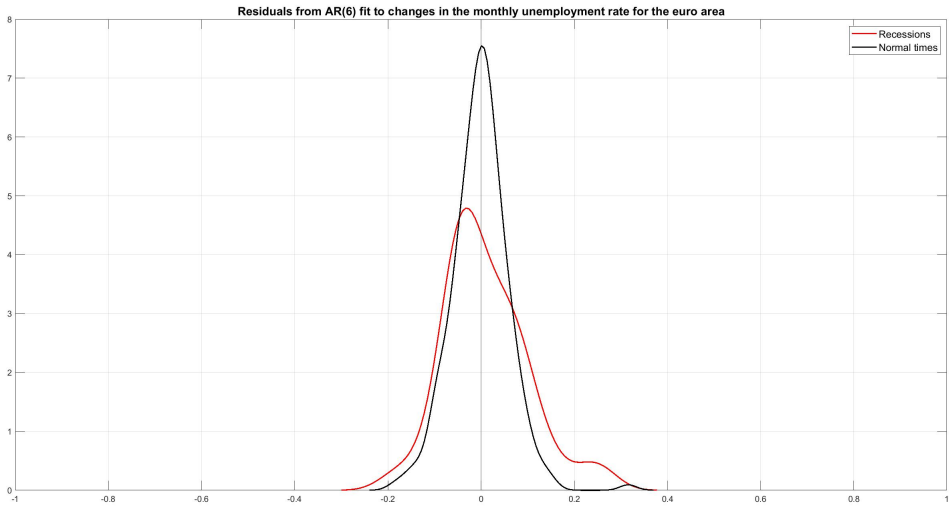

Residuals from AR(6) fit to changes in the monthly unemployment rate for the euro area

Notes: The figure shows the estimated distribution of the residuals of an autoregressive model for the changes in the unemployment rate in the euro area for recession periods, identified by the EABCN and for normal times.

Figure 22: Residuals from autoregressive fit to changes in the unemployment rate in the US distinguishing recessions form normal times

Residuals from AR(4) fit to changes in the monthly unemployment rate for the US

Notes: The figure shows the estimated distribution of the residuals of an autoregressive model for the changes in the unemployment rate in the US for recession periods, identified by the NBER and for normal times.

Figure 23: Squared and cubed residuals from autoregressive fit to changes in the unemployment rate in the euro area
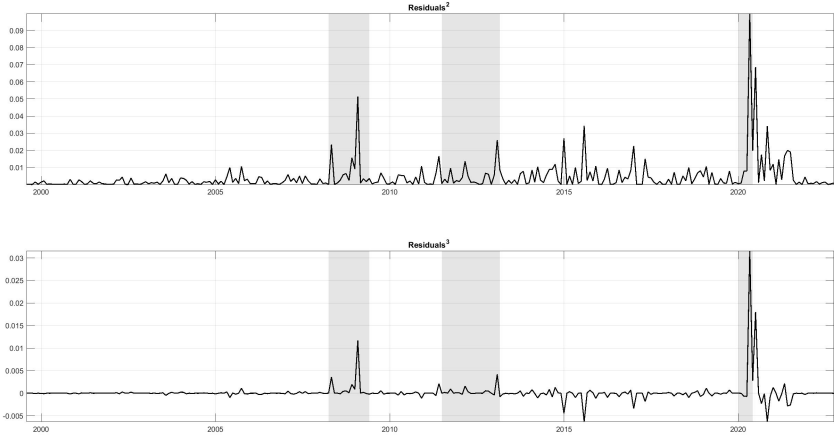

Notes: The figure shows the time series of the squared and cubed residuals from autoregressive model to changes in the unemployment rate in the euro area. The shadow bands indicate the EACN recessions periods.

Figure 24: Residuals from autoregressive fit to changes in the unemployment rate in the US distinguishing recessions form normal times
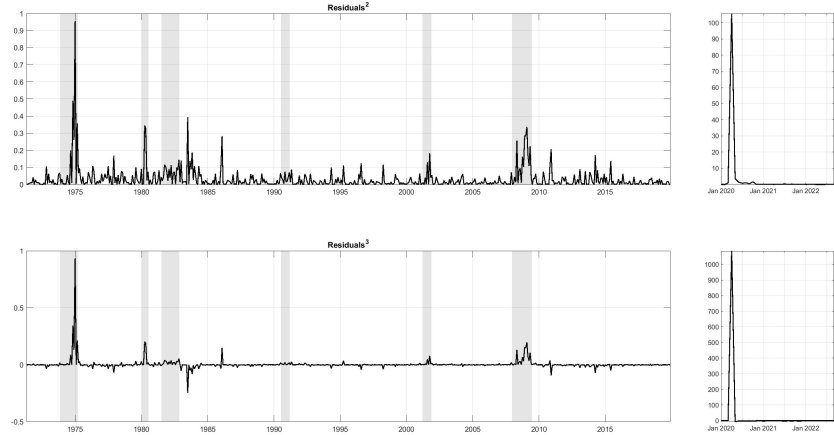
Notes: The figure shows the time series of the squared and cubed residuals from autoregressive model to changes in the unemployment rate in the US. The shadow bands indicate the NBER recessions periods.

Figure 25: *Standard normal* and *Skew normal* distributions
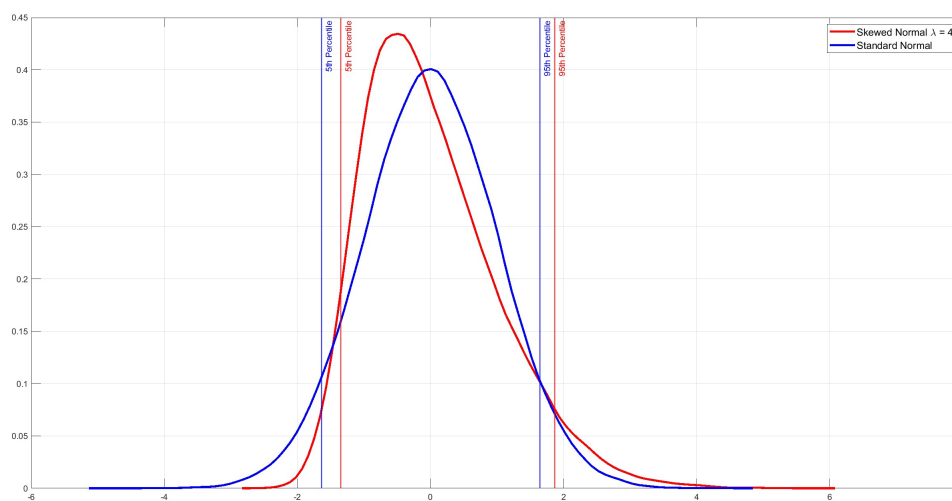
Notes: The figure shows the Standard normal distribution together with the Skew normal distribution with shape parameter $\lambda = 4$ re-parameterized to have zero mean and unit variance.

A.7 Additional tables

Table 7: Percentiles of $U_{t+h} - U_t$

Percentiles	Euro Area			United States		
	$h = 1$	$h = 3$	$h = 12$	$h = 1$	$h = 3$	$h = 12$
10%	-0.11	-0.28	-0.94	-0.23	-0.43	-1.12
15%	-0.09	-0.25	-0.89	-0.18	-0.33	-0.91
20%	-0.08	-0.23	-0.84	-0.15	-0.28	-0.81
25%	-0.07	-0.20	-0.80	-0.12	-0.24	-0.69
50%	-0.03	-0.09	-0.36	-0.01	-0.06	-0.29
75%	0.03	0.06	0.34	0.10	0.13	0.38
80%	0.05	0.13	0.51	0.13	0.20	0.83
85%	0.07	0.18	0.70	0.17	0.33	1.27

Notes: The table shows the percentiles of the distribution of the month on month, quarter on quarter and year on year changes in the unemployment rate for the euro area and the United States.

Vasco Botelho
European Central Bank, Frankfurt am Main, Germany; email: vasco.botelho@ecb.europa.eu

Claudia Foroni
European Central Bank, Frankfurt am Main, Germany; email: claudia.foroni@ecb.europa.eu

Andrea Renzetti
University of Bologna, Bologna, Italy; email: andrea.renzetti2@unibo.it